Buffer optimisation for an improved cell separation using Acoustophoresis with Polystyrene particles, Jurkat, MCF-7 and DU-145 cell lines

by Lovisa Silversand

Master's thesis in Biomedical Engineering

LUND
UNIVERSITY

Faculty of Engineering LTH
Deparment of Biomedical Engineering

Supervisor Dr. Thierry Baasch
Co-supervisor Dr. Andreas Lenshof
Examinator Pr. Thomas Laurell

Autumn 2023

Abstract

Acoustophoresis is the migration of particles/cells under the influence of sound. Particle and cell separation is an application that can be performed by acoustophoresis. This is an important technique since it can reveal important information about diseases and cells and thereby possibly improve the choice of treatment in healthcare. By utilizing sound, cells and particles in a suspension can be separated due to their distinct properties such as size, compressibility and density. The last two are parameters found in the acoustic contrast factor. The sign of the contrast factor determines the direction of the migration, which is an important factor in the separation. This thesis aims to improve the the separation between cells, using Polystyrene particles as reference. This is done by adjusting properties affecting the acoustic contrast factor, in this case the buffer conditions. By measuring the mobility ratio of cells and particles, which is based on their trajectories in the acoustophoresis chip, the buffer conditions can be analysed in an efficient way. This thesis includes tests of Polystyrene particles with different sizes and three different cell lines (DU-145 (prostate cancer cells), MCF-7 (breast cancer cells) and Jurkat (T lymphocyte cells)). During the experiments, it was found out that the MCF-7 cells exerts a change in contrast factor when suspended in a buffer with 10% and 20% Iodixanol, enabling a fully separation from the 7.79μm Polystyrene particles. It was also clear that the buffer condition had an impact of the separation since a higher density medium improved the separation for all cell lines.

Swedish/svenska
Akustophores är rörelse av partiklar/celler under inverkan av ljud. Partikel- och cell separation är en applikation som kan utföras av akustophores. Detta är en viktig teknik eftersom den kan avslöja viktig information om sjukdomar och celler och därigenom förbättra valet av behandling inom sjukvården. Genom att utnyttja ljud, så kan celler och partiklar i en lösning separeras efter deras specifika egenskaper; storlek, densitet och kompressibilitet. De två sistnämnda återfinns båda i den akustiska kontrast faktorn. Tecknet på den akustiska kontrast faktorn bestämmer riktningen på rörelsen, och är således en viktig faktor i separationen. Denna avhandling syftar till att förbättra separationen mellan celler med hjälp av Polystyrene partiklar som referens. Detta görs genom att justera egenskaperna som påverkar den akustiska kontrast faktorn, i detta fall egenskaperna hos bufferten. Genom att mäta mobiliteten hos celler och partiklar, vilket är baserad på deras banor i akustophoreschippet, kan buffertegenskaperna analyseras på ett effektivt sätt. Denna avhandling inkluderar tester med Polystyrene partiklar i olika storlekar och ett antal olika cell liner, (DU-145 (prostatacancer celler), MCF-7 (bröstcancer celler) and Jurkat (T-lymfocyt celler)). Under testerna, så blev det klart att MCF-7 cellerna erhåller en ändring i kontrastfaktorn när de är i en buffert med 10% och 20% Iodixanol, vilket möjliggör en full separation från 7.79μm Polystyrene partiklarna. Det blev också klart att egenskaperna av bufferten hade en inverkan eftersom en buffert med högre densitet påverkade separationen för samtliga cell linjer.

Popular science article

Buffer optimisation for an improved cell separation using Acoustophoresis

Acoustophoresis is a technique in microscale systems where sound is utilized to move particles and cells. When the channel width of the microchip is dimensioned to half a wavelength, a pressure node in the middle of the chip is created. This enables separation between particles and cells when suspended in a buffer medium. The separation is dependent on inherent properties of the particle/cell such as density and compressibility; factors contributing to the acoustic contrast factor. A positive sign of the contrast factor will create movement to the pressure node (middle) and a negative contrast factor creates movement to the pressure anti-nodes (sides) of the chip. The size is also of great importance since larger particles are affected by a greater acoustic radiation force, creating a faster movement towards the pressure node compared to smaller ones. By using different outlets in the acoustophoresis channel, cells and particles can efficiently be separated from each other based on their acoustic properties. A successful separation is desirable since it can reveal important information about diseases and different cell types, such as cancer cells and different breast cancer cell lines. This could lead to more personalized treatment in healthcare since a better understanding of how the different cell types work and behave is gained.

Further, it is shown that the buffer medium has an influence on the cell separation. This, since the buffer medium has an impact on the acoustic contrast factor, which affects the movement of the particles/cells in the chip. By measuring the mobility ratio, the trajectories of particles and cells in the chip can be predicted. Therefore, measuring the mobility ratio is an important tool when investigating how the buffer conditions affect the separation. A higher mobility ratio indicates a better separation between the different particles/cell types. For this thesis, the goal was to find a buffer media that could increase cell separation. This was done by investigating different buffer mediums and eventually calculating the mobility ratio using MATLAB. The cell lines that were studied during this thesis were MCF-7 (breast cancer cells), DU-145 (prostate cancer cells) and Jurkat (T-Lymphocyte cells). These were tested together with Polystyrene particles of different sizes and colors. The buffer medium was changed by adding different concentration of a dense medium.

The most important finding was that the buffer medium indeed had a great impact on the separation. A general trend that could be seen was that the higher density of the buffer, the better separation. Regarding the MCF-7 cells, it was observed a change in the acoustic contrast factor when using a buffer medium with both 10-and 20% Iodixanol. This indicates that there is a possibility to separate them from other cell lines, such as the DU-145 and Jurkat cells where no switch in acoustic contrast factor could be seen. From the experiments it could also be concluded that the Polystyrene particles seem to have different material properties even though they share the same

composition. This would be good to further investigate since they are used a lot in research as reference.

The work in this thesis will hopefully come to use in further experiments and research. This, since more advanced knowledge about the behavior and properties for both the Polystyrene particles and the different cell lines is gained.

Acknowledgements

There are many people that I would like to thank for helping me during the work with my Master's thesis. Firstly, I would like to thank Professor Thomas Laurell for letting me be a part of his research group, and for the opportunity to learn more about Acoustophoresis and its applications.

I would also like to present my greatest gratitude to my supervisor Thierry Baasch and co-suporvisor Andreas Lenshof for their incredible help during this time and for always keeping the patience up and being supportive. Thank you Thierry for your great support with MATLAB and for always answering my questions with good explanations. Thank you Andreas for all the inestimable support in the lab with the set-up and for the help with the cells.

A special thanks to Cecilia Magnusson, for teaching how to culture and take care of the cells in the cell lab, and for always having a solution of how to solve a problem.

Further more, I would like to express my joy for sharing the start of this project with Olivia Hansson Rengbrandt, making the days in the lab always funny. Also, a big thanks to Alexander Edthofer for the help with the Jurkat cells and when the set-up was messy.

At last, I would like to thank Alexander Petkovski, my family and friends for their invaluable support and kindness along this journey. Thank you for always spreading joy, even during stressful times. Without you there would be no masters degree.

Lund, October 2023

Lovisa Silversand

Notations and symbols

Letter/Symbol	Description	Unit
$\overrightarrow{F}_{drag}$	Stokes' drag force	N
$\overrightarrow{F}_{rad}$	Radiation force	N
Q_{i_n}	Inlet flow rate	m^3/s
$Q_{o_{ut}}$	Outlet flow rate	m^3/s
$Q_{t_{ot}}$	The total flow rate in the channel	-
r_{i_n}	Inlet splitting ratio	-
$r_{o_{ut}}$	Outlet splitting ratio	-
E_{ac}	Acoustic energy density	Pa
k	Wavenumber	m^{-1}
$v_{p(y)}$	Velocity along the y-axis	m/s
Φ	Acoustic contrast factor	-
$\Phi_{1,2}$	Acosutic contrast factor particle 1/particle 2	-
$MR_{1,2}$	Mobility ratio of the particle 1/particle 2	-
ρ_p	Density of the particle	kg/m^3
ρ_m	Density of the medium	kg/m^3
κ_p	Compressibility of the particle	m^2/N
κ_m	Compressibility of the medium	m^2/N
Re	Reynolds number	-
u	Flow speed	m/s
μ	Dynamic viscosity of the fluid	kg/ms
a	Radius of particle/cell	-

Contents

Abstract **I**

Popular science article **III**

Acknowledgements **V**

Notations and Symbols **VII**

1 Introduction **1**

1.1 Background and introduction to microfluidics 1

1.2 The aim of this thesis 3

1.3 The set-up 3

2 Theory **5**

2.1 Microfluidics 5

2.2 Acoustophoresis 5

2.2.1 Particle separation 7

2.3 Particle separation and mobility ratio 9

2.3.1 Calculation of mobility ratio using MATLAB 11

2.3.2 Analysis with LMS algorithms in MATLAB 14

2.4 Optimisation of buffer conditions 15

3 Separation of Polystyrene particles **17**

3.1 Method 17

3.2 Results 18

3.2.1 Separation of red 4.99μm and green 7.81μm Polystyrene particles 18

3.2.2 Separation of red 9.89μm and green 5.19μm Polystyrene particles 19
3.2.3 Separation of red 9.89μm and green 7.81μm Polystyrene particles 20
3.2.4 Comparison with earlier experiment 21
3.3 Discussion 22

4 Separation of cell lines 25

4.1 Cancer and cell lines 25
4.2 Cell culture and handeling 26
4.3 Method 27
4.4 Results and discussion 28
4.4.1 DU-145 cell line 28
4.4.1.1 Separation with DU145 and 9.89μm Polystyrene particles 29
4.4.1.2 Separation with DU145 and 7.81μm Polystyrene particles 35
4.4.1.3 Discussion 36
4.4.2 MCF-7 cell line 37
4.4.2.1 Separation of MCF-7 and 7.79μm Polystyrene particles in PBS 37
4.4.2.2 Separation of MCF-7 and 7.79μm Polystyrene particles in 10 and 20% Iodixanol 39
4.4.2.3 Discussion 40
4.4.3 Jurkat cell line 41
4.4.3.1 Separation of Jurkat cells and 7.79μm Polystyrene particles in PBS 41
4.4.3.2 Separation of Jurkat cells and 7.79μm Polystyrene particles in 10% Iodixanol 42
4.4.3.3 Separation of Jurkat cells and 7.79μm Polystyrene particles in 20% Iodixanol 44
4.4.3.4 Discussion 45

5 Conclusions and Future Directions 47

5.1 Overarching conclusions 47
5.2 Future aspects 48

References **49**

A Figures Jurkat cells **51**

B Figures MCF-7 cells **53**

C Figures DU-145 cells **55**

1 Introduction

· In the first chapter there is an overview and introduction to the microfluidic and acoutsophoresis area. The aim of the thesis is also stated. This chapter provides with an introduction into the world of microfluidics.

· In the second chapter the theory, the technique behind acoustophoresis and the concept with mobility ratio is explained and stated. This chapter aims to increase the understanding in how mobility ratio relates to the particle/cell separation and how it can be used to improve it.

· In the third chapter the separation with Polystyrene particles is. The method, result and important findings are presented.

· In the fourth chapter the separation with the different cell lines is. The method, result and important findings are presented.

· In the fifth chapter the important findings from the experiments are concluded and possible future outlook are discussed.

The experiments with the Polystyrene particles and DU-145 cell line are done in collaboration with another master student, Olivia Hansson Rengbrandt. The experiments with the MCF-7 and Jurkat cell lines are individually chosen for this thesis.

1.1 Background and introduction to microfluidics

Microfluid is a fast growing field in research and has been groundbreaking for the technological development in biochemistry. It has enable us to gain more knowledge about complex biological processes and diseases and hence paved the way for individual-specific treatments and much faster sample analysis (Song et al., 2014). When operating in microscale systems fluid start to behave differently. This enables a precise control over the liquid flow in channels since the flow in channel starts to appear laminar due to a low Reynolds number, generating a more efficient analysis (Lenshof and Laurell, 2010). Beyond this, the advantages with microfluidics is many, including that the sample and reagent volume can be reduced making it very cost effective (Regmi et al., 2022).

Acoustophoresis is an microfluidic application where sound is utilized to manipulate particles or cells in fluids in microscale systems. When particles or cells in a buffer medium suspension are exposed to an acoustic sound wave field, they will be influenced by an acoustic radiation force. Movement of particles in the sound field is induced if the acoustic properties between the buffer medium and particles differ. The direction of movement is dependent on properties as compressibility and density of the buffer

medium and particle/cell (Nilsson et al., 2004).

By putting the main channel width of the acoustophoresis chip to half a wavelength a pressure node in the middle of the chip is created. This results in that some particles will move to the pressure anti-nodes of the chip and some particles will move to the pressure node. Particles/cells with a positive contrast factor will move to the pressure node and particles/cells that exhibits a negative contrast factor will move towards the pressure anti-nodes. If the buffer medium is more dense than the particles/cells and the compressibility of the buffer medium is low, it will typically display a negative contrast factor and movement to the pressure anti-nodes occurs. By splitting the end of the flow channel to different outlets, particle/cell separation is enabled (Laurell, 2021a). The purity of the acoustic separation can further be determined by using flow cytometry.

When performing particle separation using acoustophoresis the buffer conditions are of great importance for improvement of the separation efficiency (Urbansky, 2019). That is because the acoustic radiation force is dependent on the acoustic contrast factor, and the contrast factor is dependent on the density of the buffer medium. Since the mobility ratio is related to the acoustic contrast factor, measuring the mobility ratio of cells/particles is a tool that can be explored to improve the buffer conditions and thereby increase the particle separation. The mobility ratio is found to be the individual parameter that provides to the trajectories of the cells/particles in the acoustophoresis chip. The trajectory is an inherent property of the cells/particles independent of factors such as flow rate, acoustic energy density, channel length and fluid viscosity. By using the mobility ratio, the particle/cell path can be predicted which provides an open field for optimising parameters such as the buffer conditions (Péroux, 2022).

Acoustophoresis is a contact and label free technique which can be used in other areas than particle separation, such as particle washing (Laurell, 2021a), where particles are transported from one buffer medium to another buffer medium without any mixing of the different buffers. This method is efficient to use when there is a need to remove contaminates in the sample (Urbansky, 2019). Particle separation using microfluidic devices could potentially have a great impact in diagnostic and treatment within medicine. For example, CTC (circulating tumor cells) can be separated from blood and give useful information about how to choose the best therapeutic treatment (Li et al., 2015). It is also possible to separate different subtypes of cells, e.g. lymphocytes, monocytes and granulocytes populations were successfully separated with a purity over 90% (Urbansky et al., 2019).

Even though the technique holds promising possibilities for the future, there are some limitations. During a normal blood test a volume of 5-15 mL is collected from a patient. In order to achieve a high sample processing, a flow rate over 100 μl/min is required and used to be able to process the sample within one hour. The sample throughput using acoustophoresis is for now limited to 5-20 μl/min (Péroux, 2022). This means that the sample throughput currently not match the requirements for a quick sample analysis with a high throughput. An increased flow rate would affect the flow dynamics since inertia effects starts to appear. Due to possible spill over, the particle separation deteriorates since all of the particles are pushed into the center outlet (Undvall et al., 2022). However, these effects follows with the high throughput and does not influence this study where the experiments are performed at much lower flow rates.

1.2 The aim of this thesis

The aim with this thesis is to investigate and optimise the buffer conditions to increase the cell-cell separation when performing acoustophoresis. This is done by evaluating the mobility ratio of different cell lines using fluorescent Polystyrene particles with different sizes as a reference.

In this thesis three different cell lines are used:
· DU-145 cell line (prostate cancer cells)
· MCF-7 cell line (breast cancer cells)
· Jurkat cell line (T-lymphocyte cells)

1.3 The set-up

For performing particle separation using acoustophoresis an experimental setup is needed. The setup used in this thesis is shown below in figure 1.1 and 1.2.

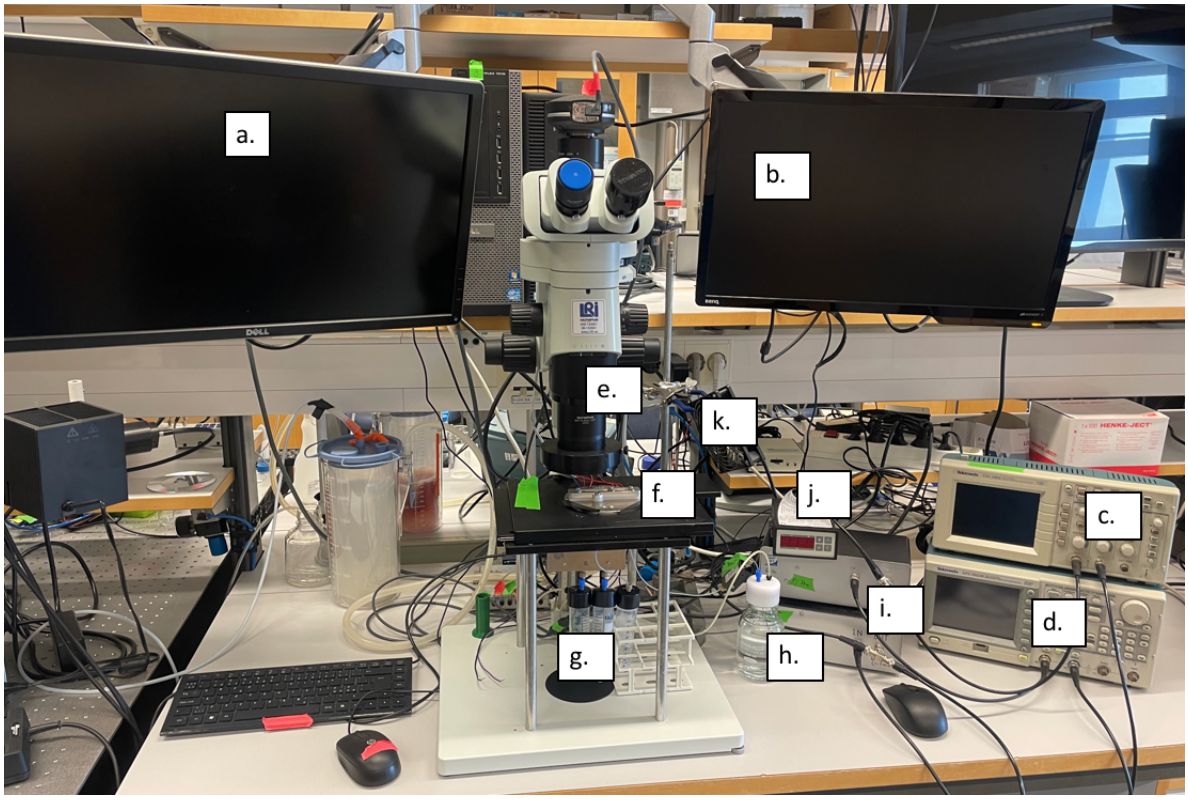

Figure 1.1: (a) Monitor showing the acoustophoretic chip (b) Monitor showing the flow control settings (c) Oscilloscope (d) Signal generator (e) Microscope (f) Acoustophoresis chip (g) Sample tubes for sample inlet, side outlet, center outlet (h) Buffer (i) Amplifiers (j) Thermometer showing the temperature (k) Pressure driven system.

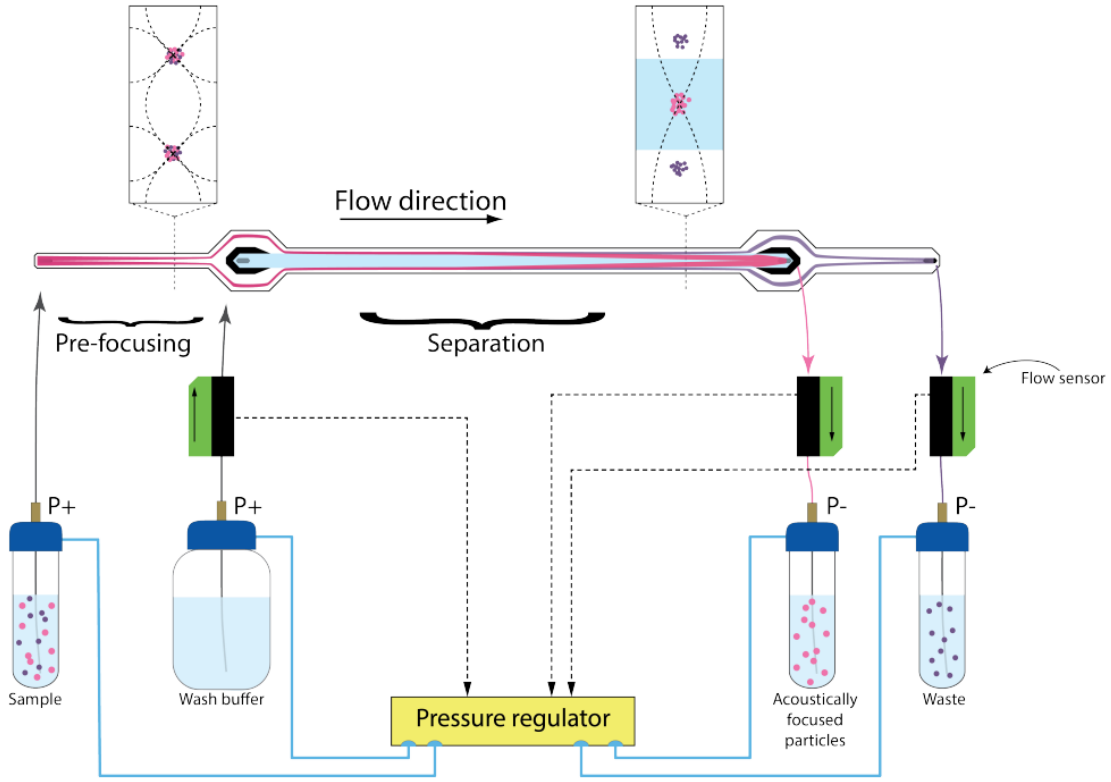

Figure 1.2: Schematic view over the set-up. The sample enters through the pre-focusing channel and is later mixed with wash buffer before entering the separation channel. The flow is regulated by a pressure driven system and flow sensors. Figure (Laurell, 2021b)

The flow is controlled and regulated by a pressure driven system and flow sensors. The flow parameters are adjusted via an in-house Labview code.

2 Theory

2.1 Microfluidics

When operating at microscale level fluid flows starts to behave differently. Reynolds number is used to describe and characterize the fluid flow. It is a dimensionless number which gives the ratio between the inertial and viscous forces. The two types of fluid dynamics are turbulent and laminar flow.

Reynolds number is defined as

$$Re = \frac{\rho \cdot u \cdot L}{\mu} \tag{2.1}$$

where Re is Reynolds number, ρ the density of fluid, μ the dynamic viscosity of the fluid, L the characteristic linear dimension and u the characteristic flow speed.

A low Reynolds number indicates laminar flow and the fluid will flow in distinct streamlines and inertial forces will be inconsiderable comparing with the viscous forces. Typically Reynolds number is less than one when using microfluidic devices since the channel length scale is so small. This property is utilized in microfluidics since it enables manipulation of fluid and great control over particles in fluid (Shanko et al., 2019).

2.2 Acoustophoresis

When superimposing two acoustic standing waves with opposite propagation direction but same frequency and amplitude, acoustic standing waves can be established. The acoustic standing waves are driven by transducers acting on the chip (Lenshof, 2008).

The resonance in the channel builds up a strong acoustic field creating forces. The pressure field of a one dimensional acoustic standing wave can be described as

$$p_1 = p_a \cdot \cos(k \cdot y \cdot t) \tag{2.2}$$

where p_a represents the amplitude of the first order pressure field, y as the position of the particle, t as time, and k=$\frac{2 \cdot \pi}{\lambda}$ represents the wave number.

Furthermore, particles in suspension will be affected by an acoustic radiation force that induces movement of the particles. The radiation force is given by

$$\overrightarrow{F}_{rad} = -4\pi\Phi ka^3 E_{ac} sin(2ky) \cdot \overrightarrow{y} \tag{2.3}$$

where a is the radius of the particle, E_{ac} the acoustic energy density and Φ the contrast factor of the particle defined as

$$\Phi = \frac{5 \cdot \rho_p - 2 \cdot \rho_m}{2 \cdot \rho_p + \rho_m} - \frac{\kappa_p}{\kappa_m} \tag{2.4}$$

The acoustic contrast factor Φ is dependent on the density of the particle ρ_p and density of the medium ρ_m, compressibility of the particle κ_p and compressibility of the medium κ_m. The resulting sign of the contrast factor determines weather the particle will move towards the pressure anti-node or pressure node. Particles with a contrast factor less then zero will move towards the pressure anti-node and greater than zero towards the pressure node, see figure 2.1 and 2.3.

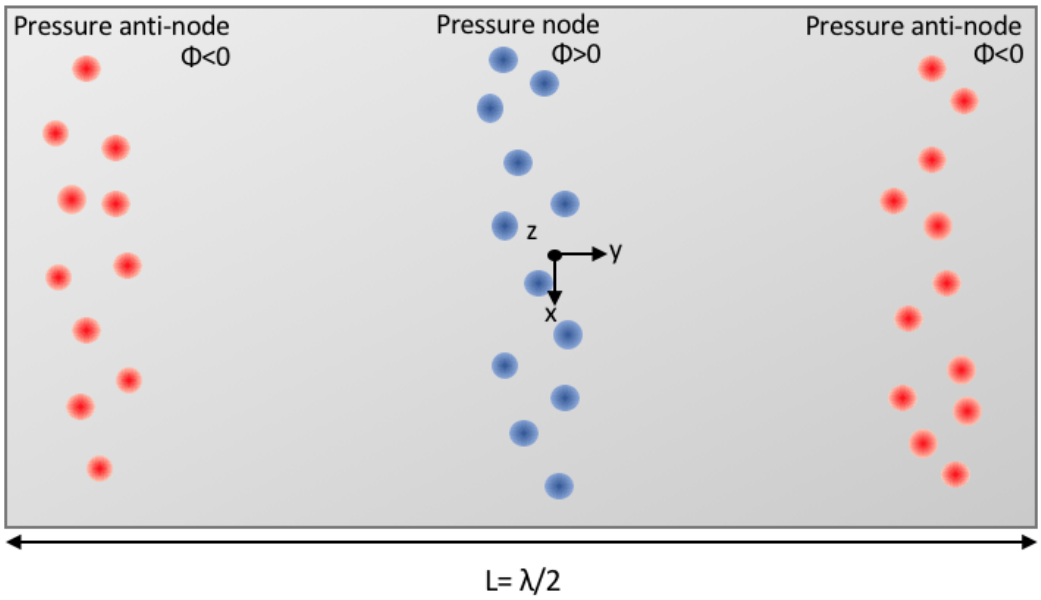

Figure 2.1: Illustration of the cross section in the acoustophoresis chip with an acoustic standing wave. Particles (blue) with a contrast factor greater than zero moves towards pressure node and particles (red) with a contrast factor less than zero moves towards the anti-nodes.

The acoustic energy density E_{ac} found in equation 2.3 is given by

$$E_{ac} = \frac{p_a^2}{4 \cdot \rho_m \cdot c^2} \tag{2.5}$$

where ρ_m is the density of the medium, c speed of sound in the medium.

2.2.1 Particle separation

The acoustophoresis chip used in all experiments in this thesis has a main channel (separation channel) width of 375 μm and the pre-focusing channel has a width of 300 μm. An illustration of the acoustophoresis chip can be seen in figure 2.2.

The sample enters via sample/side inlet to the pre-focusing channel and is exposed to a 5 MHz transducer. Here the particles are aligned and focused in two dimensions before entering the main channel. The buffer medium enters through buffer/center inlet. In the main channel the particle separation takes place. The particles are affected by a 2 MHz transducer and are sorted due to their acoustic properties in order to enter different outlets collects. The largest particles are collected via center outlet and the smaller particles are collected via side outlet due to their difference in acoustic mobility.

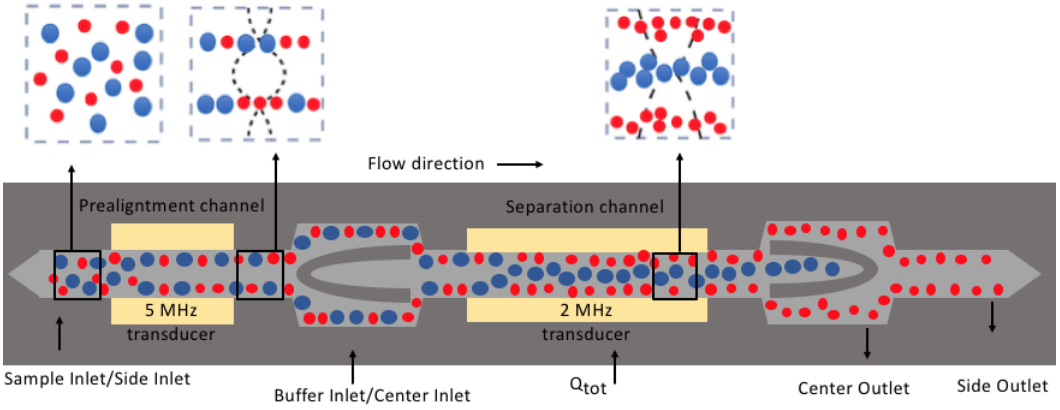

Figure 2.2: Overview of the 2D acoustophoresis chip. The particles enter through side inlet and are pre-focused under the influence of a 5MHz transducer. The particles are aligned into two distinct streamlines, giving them the positions (x,y,z). In the separation channel particles are separated based on their acoustic properties and are collected into two different outlets.

When particles or cells enter the pre-focusing channel they are arranged so that they all have the same starting position (x,y,z) when entering the separation channel. This is important and makes sure that the separation in the main channel is only due to their differences in acoustic properties, size and compressibility (Jakobsson et al., 2014).

Particles and cells that are located inside the acoustophoresis chip will be exposed to an acoustic field. This creates forces acting on the particles. Depending on size and difference in acoustic contrast factors, the force acting on the particle will be different. Particles that are larger in size will be affected by a larger acoustic radiation force, see figure 2.3. This causes the particles to have a higher acoustic mobility, and hence they travel faster into the center while the smaller will be further to the sides in the acoustic chip, due to a slower motion (Lenshof and Laurell, 2011). If the lateral gap between the two species is sufficiently large they can be collected into two different outlets.

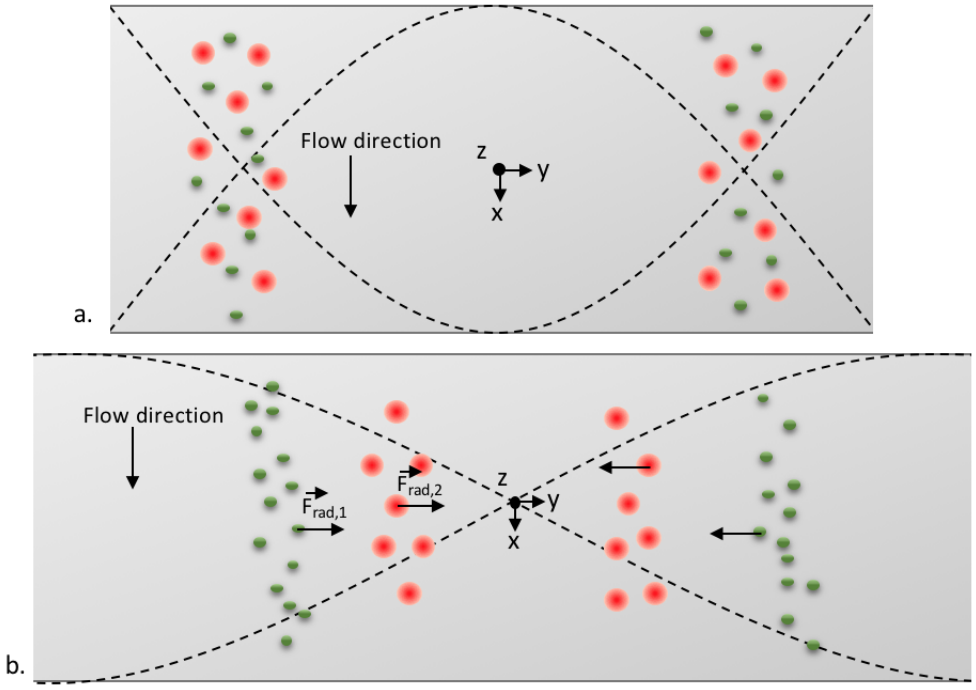

Figure 2.3: a. Top view of the prefocusing channel. The particles are focused into two distinct streamlines before entering the main channel. Channel width equals the wavelength of one acoustic standing wave b. Illustrates the top view of the main channel. The wavelength is put to twice the width of the channel. Bigger particles (red) are effected by a stronger radiation force than the smaller particles (green) and travel faster towards the channel center. This enables particle separation.

The total flow in the main channel Q_{tot} can be expressed as

$$Q_{tot} = Q_{s.in} + Q_{c.in} = Q_{s.out} + Q_{c.out} \tag{2.6}$$

where $Q_{s.in}$ is the flow rate in side inlet, $Q_{c.in}$ flow rate in center inlet, $Q_{s.out}$ flow rate in the side outlet and $Q_{c.out}$ the flow rate in the center outlet.

The flow rate in the channel is an important parameter for the particle migration. With a lower flow rate the particles will migrate in a slower manner resulting in a better separation. The flow rate is adjusted when running with cells, and usually the flow rate is significant lower comparing to when using particles. This is because cells have lower acoustic mobility and therefore move slower towards the pressure node.

Further, the inlet split ratio is defined as

$$r_{in} = \frac{Q_{s.in}}{Q_{tot}} \tag{2.7}$$

and the outlet split ratio is defined as

$$r_{out} = \frac{Q_{s.out}}{Q_{tot}} \tag{2.8}$$

2.3 Particle separation and mobility ratio

In this thesis the method for calculating and measuring the mobility ratio is done according to earlier experiments and theory performed and used by Linda Péroux in her thesis "Pushing the boundaries of acoustic particle separation: achieving high-throughput, avoiding spillover effects, investigating the effects of the particle concentration, and measuring acoustic properties" (Péroux, 2022). This method and theory is explained below in this chaper 2.3 and in chapter 2.3.1.

A particle inside the channel will be affected by two different forces along the y-axis. The forces that will act on the particle the acoustic radiation force and Stokes' drag force, $\overrightarrow{F}_{rad}$ and $\overrightarrow{F}_{drag}$ respectively, illustrated in figure 2.4 below.

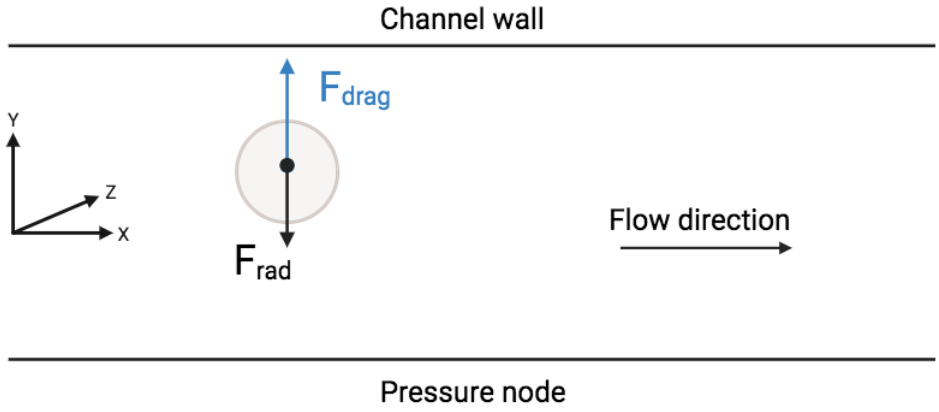

Figure 2.4: A particle inside the channel will be affected by two forces in opposite directions, $\overrightarrow{F}_{drag}$ and $\overrightarrow{F}_{rad}$. Stokes' drag force will slow down the motion of the particle while the acoustic radiation force pushes the particle against the pressure node.

The acoustic radiation force $\overrightarrow{F}_{rad}$ is expressed in equation 2.3 and arise due to the acoustic standing wave, which creates a force that affects the particle, pushing it towards the pressure node. Beyond this, the particle will be affected by Stokes' drag force, $\overrightarrow{F}_{drag}$ expressed as followed

$$\overrightarrow{F}_{drag} = -6\pi a\eta v_p(y) \tag{2.9}$$

where a is the radius of the particle, η the viscosity of the fluid and v_p the velocity of the particle along the y-axis. Stokes' drag force that will act on any particle traveling

in fluid, forcing it against its travel direction resisting the motion down as a restriction against motion.

In dynamic equilibrium and neglecting acceleration, the sum of the forces acting on the particle, F_{drag} and F_{rad} is equal to zero. The velocity of the particle in the y-axis (v_p) can be further explained by following differential equation

$$v_p(y) = -\frac{2}{3} \cdot \Phi \cdot \frac{k \cdot a^2}{\eta} \cdot sin(2ky(t)) \cdot E_{ac} \tag{2.10}$$

where Φ is the acousitc contrast factor, η the dynamic viscosity, a is the radius of particle, the wavenumber k, y the position of the particle and E_{ac} the acoustic energy density.

The mobility ratio describes how two particles move in relation to each other. In the case of two particles in the acoustic field, the mobility ratio describes how much faster particle one will reach to the pressure node comparing to particle two, when exposed to an acoustic standing wave. This can be explained by

$$MR_{1,2} = \frac{\Phi_1 \cdot a_1^2}{\Phi_2 \cdot a_2^2} \tag{2.11}$$

where Φ is the contrast factor for respective particle, and a the radius for the particle.

In order to achieve an efficient particle separation the movement of the particle is important to predict. Dr. Thierry Baasch has derived an expression where the mobility ratio relates to particle the path (published and taken from Linda Péroux report (Péroux, 2022) and it is given as follows

$$MR_{1,2} = \frac{\Phi_1 \cdot a_1^2}{\Phi_2 \cdot a_2^2} = \frac{\int_{y0}^{y_{e1}} \left(\frac{v_x(y)}{sin(2 \cdot k \cdot y)} \right) dy}{\int_{y0}^{y_{e2}} \left(\frac{v_x(y)}{sin(2 \cdot k \cdot y)} \right) dy} \tag{2.12}$$

This expression shows that the only parameters that are of importance are the initial position of the particles when prefocused, y0, and the end position of the first particle type y_{e1} and the second particle type y_{e2} in the main channel after main focusing. v_x(y) describes the flow profile of the velocity in the x-direction. Illustration of this is shown in chapter 2.3.1.

Hence, the mobility ratio can be used to predict the particle/cell path and be used as a tool to evaluate the impact of the buffer medium in order to improve the separation efficiency.

2.3.1 Calculation of mobility ratio using MATLAB

For calculation of the mobility ratio a MATLAB program was provided by Dr Thierry Baasch is used. As mentioned from equation 2.12 derived from Dr. Thierry Baasch, there are three important measuring values for calculation of the mobility ratio. The first value y_0 is measured directly at the inlet view after the particle streams are pre-focused. Illustration is shown below in figure 2.5. The value of y_0 at the inlet is taken at 0V, and the y_0 value represents the initial position for the particle.

When the particles are separated in the main channel, the final position of the particles y_{e1} and y_{e2} (representing particle stream one and particle stream two respectively) are used as input parameters in MATLAB to calculate the mobility ratio. The pictures used for determining the final positions of the particles are taken at the outlet fork, the end of the main channel.

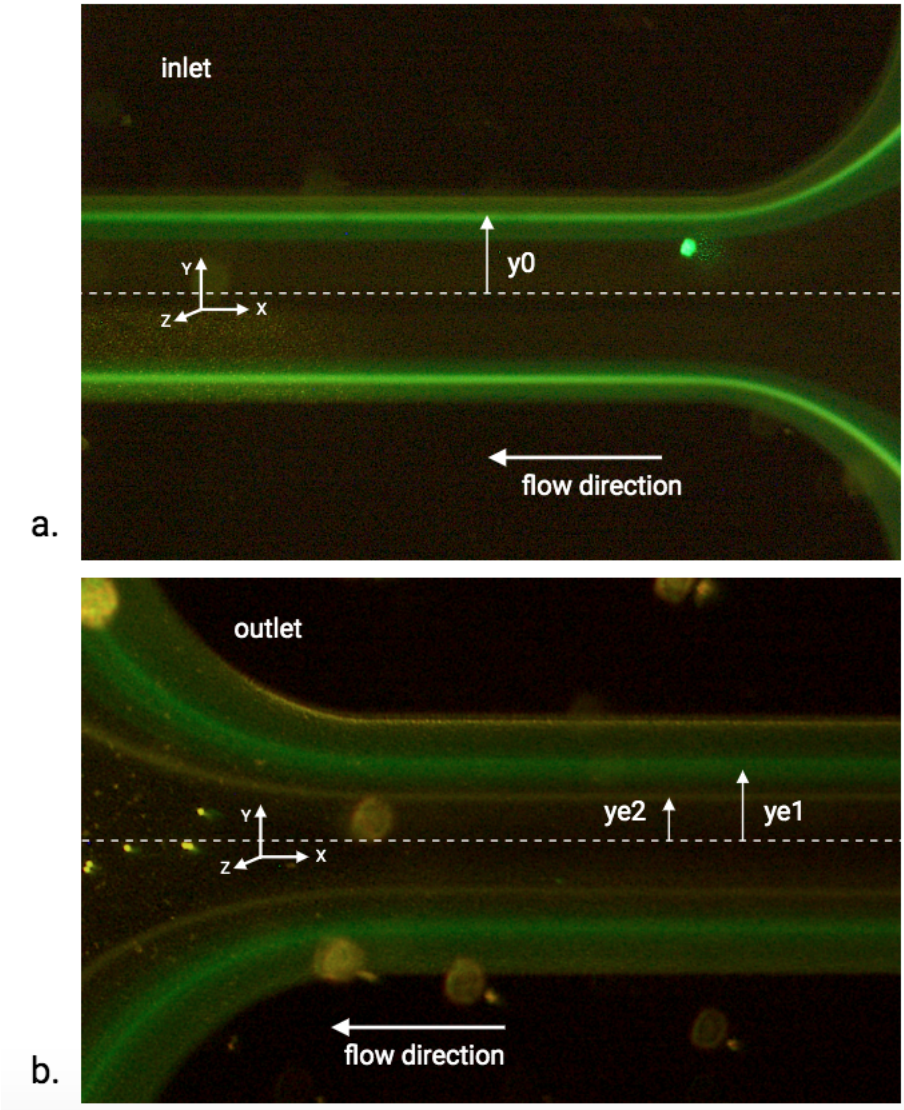

Figure 2.5: a. Showing the inlet fork at 0V for a sample with Calcein AM stained green DU-145 cells and red 9.89μm Polystyrene particles using a buffer with 20 % Iodixanol. Initial position y_0 is extracted from the image using MATLAB b. Showing the outlet fork. The DU-145 cells are stained with Calcein-AM and appears green. The orange/red particle stream is the 9.89μm Polystyrene particles. The final position, y_{e1} and y_{e2} is analysed in MATLAB.

The width of the particle streamlines corresponds to the width of the peaks that can be identified when plotting the intensity on the y-axis and number/position on the x-axis, see figure 2.6. The position of the particle/cell streamline is obtained by the distances between the two peaks for the same particel/cell type divided by two, see figure 2.7. In this way, the values for y_{e1}, y_{e2} and y_{e1} and y_0 are obtained. These values are used together with equation 2.12 in MATLAB to receive a value of the mobility ratio.

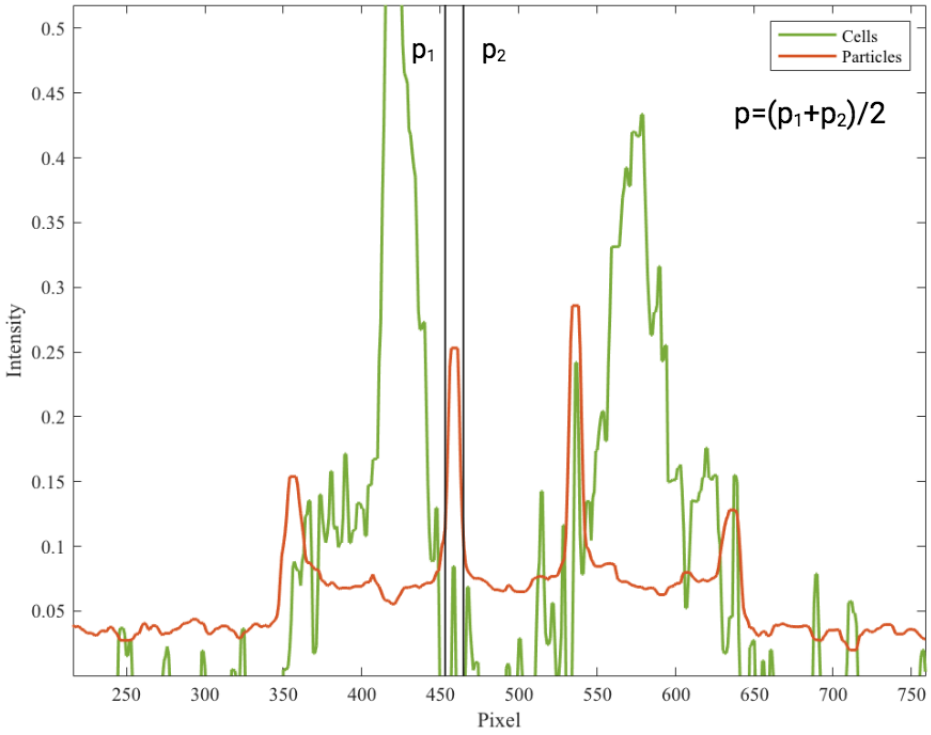

Figure 2.6: The width of the peak (distance between p1 and p2) represents the width of the cell/particle streamline. The peak position p share information about the position of the streamline (peak) in the y-axis. The width of the peak brings an uncertainty of the particle position due to the variation of cells/particles. The peak position is determined to the middle of the peak.

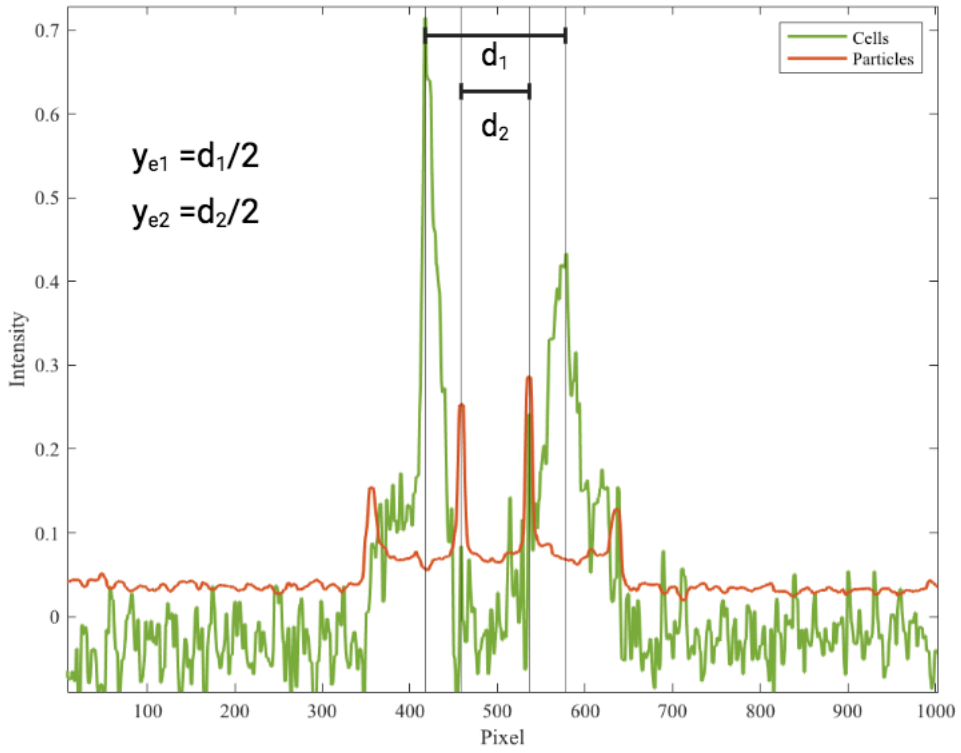

Figure 2.7: The value for the peak position is obtained by measuring the distance between the two different particle/cell streamlines (for the same type) and divide it by 2. This gives values for the different streamlines, y_{e1}, y_{e2}. The same measurement is done to receive a value of y_0.

2.3.2 Analysis with LMS algorithms in MATLAB

For some experiments the figures taken at the outlet fork were difficult to evaluate. This is mainly because the cells are seen very faint and thereby the streamlines are hard to distinguish. When running the MCF-7 cell line, a new implementation for the analysis in MATLAB was done by Dr Thierry Baasch. This implementation is done to facilitate the analysis when the streamlines are seen poorly and is built on Least mean squares algorithms (LMS).

The filtering uses that every pixel contains of three colors: green, red and blue. Since both the particles and cells have a specific color combination (red, green, blue) they both can be seen as vectors with three elements. The least mean squares algorithm is used to find the specific contribution of the cells and particles to every pixel. This can help improving the distinction between cells and particles and therefore the evaluation of the data.

This tool is used when analysing the separation between DU-145 cells and 9.89μm Polystyrene particles in 10% Iodixanol. The results are further discussed in chapter 4.4.1.1.

2.4 Optimisation of buffer conditions

One way to improve the particle and cell separation is to alter the buffer conditions. When changing the buffer conditions the density and compressibility is affected. This can be useful since it will affect the acoustic radiation force acting on the particles/cells. The larger the difference in mobility ratio between different cell/particle type, the better the separation will be. This opens a leeway to find an optimal buffer medium to improve particle separation.

Buffers used in this thesis are MQ water (for the particles), phosphate-buffered saline (PBS) (for the cells) and different percentages of Iodixanol (10%, 20%). PBS is used as buffer component in Iodixanol. Iodixanol is prepared before experiments by mixing Optiprep (60-% w/v) with 10 x phosphate-buffered saline. Optiprep serves as a density medium for the buffer solution, and the amount of it is changed to achieve a specific density of the buffer. The density of the Optiprep used is 1.320±0.001 g/mol. For the preparations of Iodixanol, see table 2.1 below.

PBS is preferred to use over MQ-water with cells since it provides a good environment for the cells and prevents it from collapse due to osmotic pressure and maintains the balance of the cells (Martin et al., 2006).

Table 2.1: Calculations for the Iodixanol solutions used in experiments.

% Iodixanol	**Optiprep 60% w/v [ml]**	**PBS [ml]**	**MQ water [ml]**
10	16.67	10	73.33
20	33.33	16.67	60

By running experiments with different buffer conditions and evaluate the acoustic mobility for the outcome, the best buffer conditions for an improved separation can be determined.

3 Separation of Polystyrene particles

The main goal of this chapter is to measure the mobility ratio of different fluorescent Polystyrene particles in different buffers. This is done to check the accuracy of the method before starting with the cell lines and to be familiar with the set-up.

3.1 Method

For the separation of Polystyrene particles, four fluorescent particles are used: Red 4.99μm, Red 9.89μm, Green 7.81μm and Green 5.19μm. They all comes from the manufacturer: Microparticles gmbh in a concentration of 2.5% w/v. They were first diluted to a concentration of 0.001% w/v, but as they were hardly visible during the first test experiment, the concentration was increased to 0.0025 % w/v. The particles were added into a solution (with buffer) giving a total volume of 5mL.

For the separation of Polystyrene particles two different buffers were used: MQ water and a buffer with 20% Iodixanol. The set-up used is explained in chapter 1.3, and the flow control settings were kept constant as described below in table 3.1. The frequency in the pre-focusing channel was held close to 5 MHz and the frequency in the main channel close to 2 MHz.

The measuring method used is described in chapter 2.3.1. The analysis is based on that some data points are more precise than others. The analysis is limited to the data points that are close to the maximal gap using the quadratic fit. The method tries to find the maximum gap in order to improve the accuracy, and takes an average of those values which are close to the maximum. This method is used when creating the separation curves, shown below in section 3.2.

Table 3.1: The parameters used when performing the experiments with the Polystyrene particles.

Parameter	**Value**
r_{in}	0.8
r_{out}	0.2
Total flow rate [μl/min]	200
Camera exposure time [s]	0.5-1
Temperature [C°]	23-25

Three pictures were taken for every voltage, starting from 0V. Also, three figures were taken at the inlet at 0V and at the end to be make sure that the experiment went

successful.

3.2 Results

Below the results for the tests with the different Polystyrene particles are presented.

3.2.1 Separation of red 4.99μm and green 7.81μm Polystyrene particles

The mobility ratio between the red 4.99μm and green 7.81μm Polystyrene particles is assessed in two different buffers: MQ water and 20% Iodixanol. The separation curve that was obtained is shown in figure 3.1 and the mobility ratios are stated in table 3.2. The separation curve shows the data points obtained for the different buffers. The gap distance is the distance between the two different particle/cell streamlines for the same voltage. The mobility ratio indicates how well the separation went, where a larger value represents a better separation.

For the run in MQ water the amplitude in the main channel was swept between 0 and 9.5V and for the run in 20% Iodixanol it was swept between 0 and 14V. The amplitude is altered 0.5-1V at once in steps.

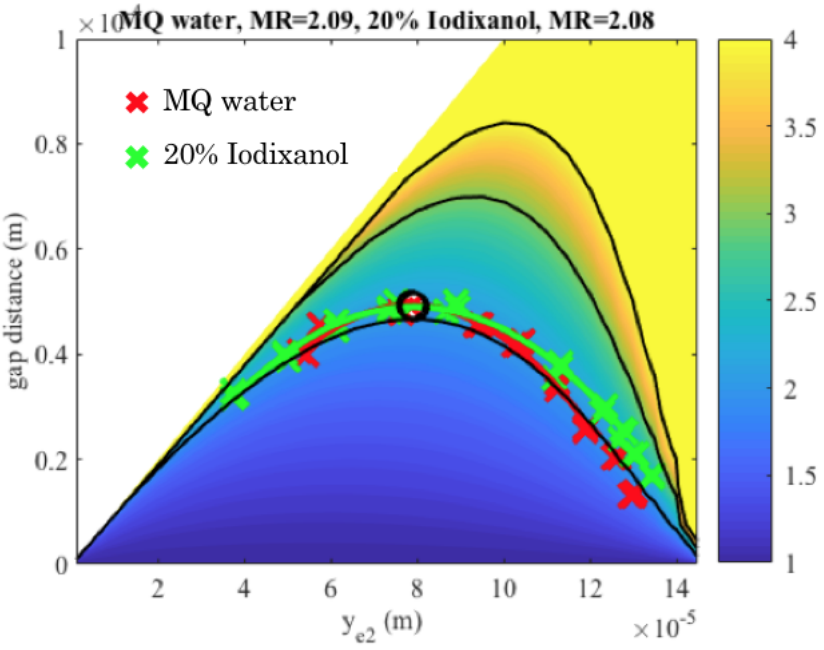

Figure 3.1: Showing the separation curve for the 4.99μm and 7.81μm Polystyrene particles in MQ water and 20% Iodixanol. The black circles represents the maximum values.

Table 3.2: Showing the mobility ratios for the Polystyrene particles (4.99μm/7.81μm) in MQ water and 20% Iodixanol using the analysis with quadratic fit.

Buffer	Mobility ratio	Max Mobility ratio	Min mobility ratio
MQ water	2.09	2.2	1.91
20% Iodixanol	2.08	2.32	2.01

3.2.2 Separation of red 9.89μm and green 5.19μm Polystyrene particles

The mobility ratio between the red 9.89μm and green 5.19μm Polystyrene particles is assessed in two different buffers: MQ water and 20% Iodixanol. The separation curve that was obtained is shown in figure 3.2 and the mobility ratios are stated in table 3.3.

For the both of the runs (MQ water and 20% Iodixanol) the amplitude in the main channel was swept between 0 and 18V with steps of 0.5-1V.

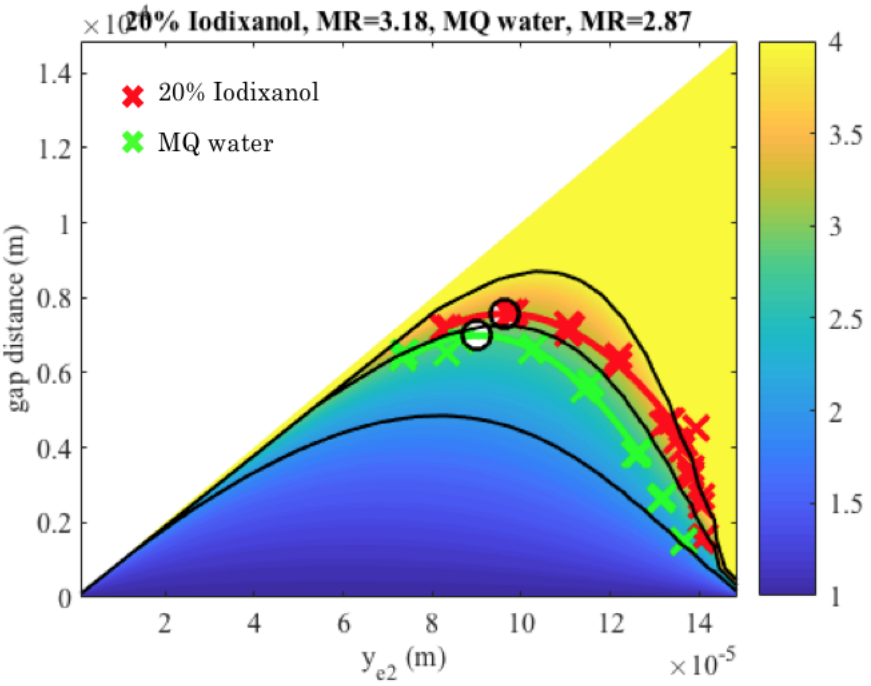

Figure 3.2: Showing the separation curve for the 9.89μm and 5.19μm Polystyrene particles in MQ water and 20% Iodixanol. The black circles represents the maximum values. The black lines represents different isolines.

Table 3.3: Showing the obtained mobility ratios for the Polystyrene particles (9.89μm /5.19μm) in MQ water and 20% Iodixanol using the analysis with quadratic fit.

Buffer	Mobility ratio	Max Mobility ratio	Min mobility ratio
MQ water	2.87	2.99	2.51
20% Iodixanol	3.18	4.98	3.13

3.2.3 Separation of red 9.89μm and green 7.81μm Polystyrene particles

The mobility ratio between the red 9.89μm and green 7.81μm Polystyrene particles is assessed in two different buffers: MQ water and 20% Iodixanol. For the run in MQ water the amplitude in the main channel was swept between 0 and 12V and for the run in 20% Iodixanol it was altered between 0 and 20V.

During both of the runs, there was a fiber located in the outlet fork that may have affected the results. This is shown for the run in MQ water, see figure 3.3 and 3.4 below.

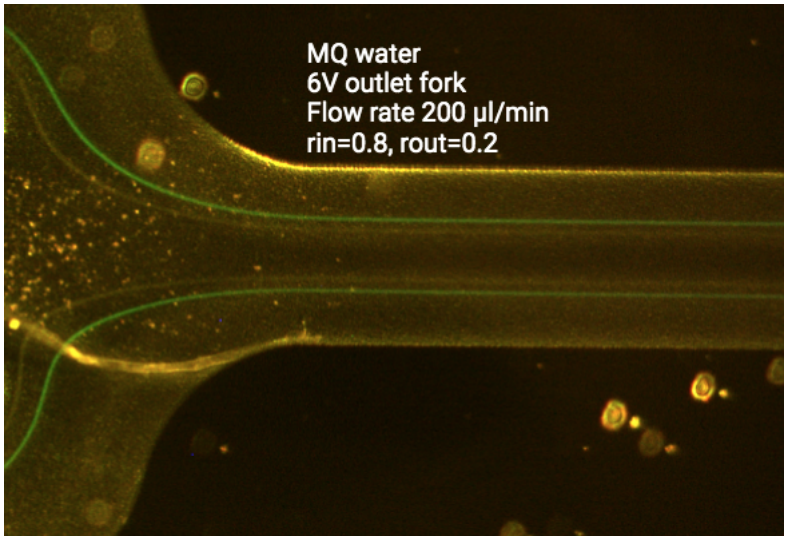

Figure 3.3: Showing the outlet fork for the red 9.89μm and green 7.81μm Polystyrene particles in MQ water at 6V with a fiber located at the outlet.

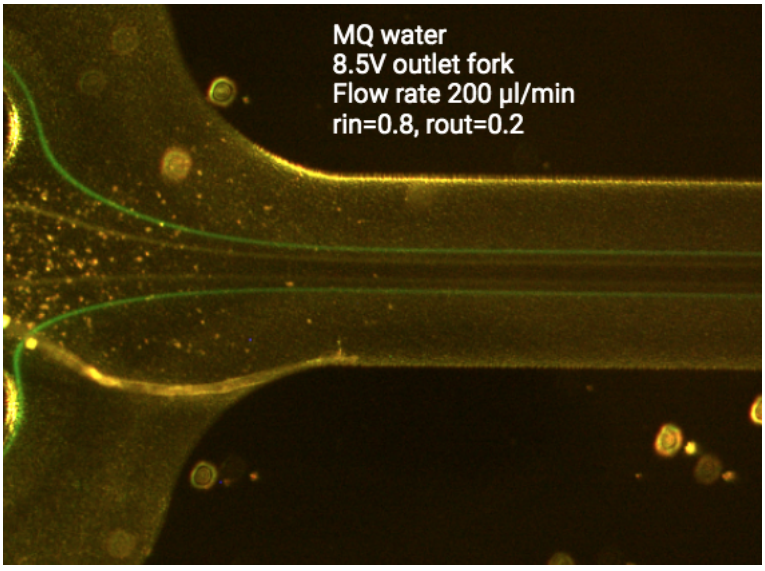

Figure 3.4: Showing the outlet fork for the red 9.89μm and green 7.81μm Polystyrene particles in MQ water at 8.5V with a fiber located at the outlet.

The separation curve that was obtained is shown in figure 3.6 and the mobility ratios are stated in table 3.4.

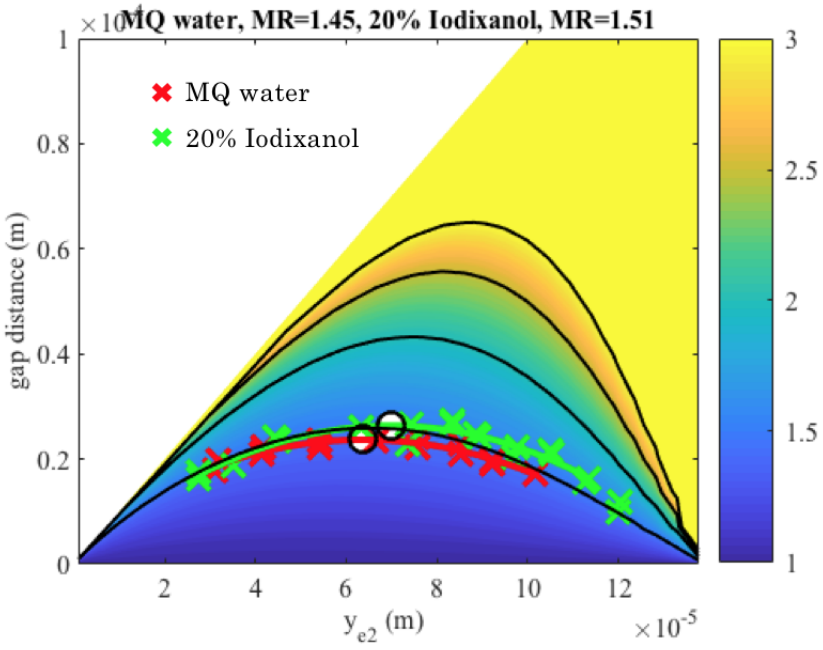

Figure 3.5: Showing the separation curve for the 9.89μm and 7.81μm Polystyrene particles in MQ water and 20% Iodixanol. The black circles represents the maximum values.

Table 3.4: Showing the obtained mobility ratios for the Polystyrene particles (9.89μm/7.81μm) in MQ water and 20% Iodixanol using the analysis with quadratic fit.

Buffer	Mobility ratio	Max Mobility ratio	Min mobility ratio
MQ water	1.45	1.52	1.43
20% Iodixanol	1.51	1.64	1.44

3.2.4 Comparison with earlier experiment

Particle separation with similar Polystyrene particles were performed earlier by Linda Péroux (Péroux, 2022). A method that can show a high repeatability could potentially be concluded as a trustful method to use, and therefore the results from this thesis are compared with the data from Linda Péroux thesis (Péroux, 2022).

The mobility ratios obtained from this thesis are compared with the mean value of Linda's three repeated experiment. The comparison is shown below in figure 3.6, where Linda's values for the mobility ratio is mentioned as reference value and the work for this thesis as thesis value.

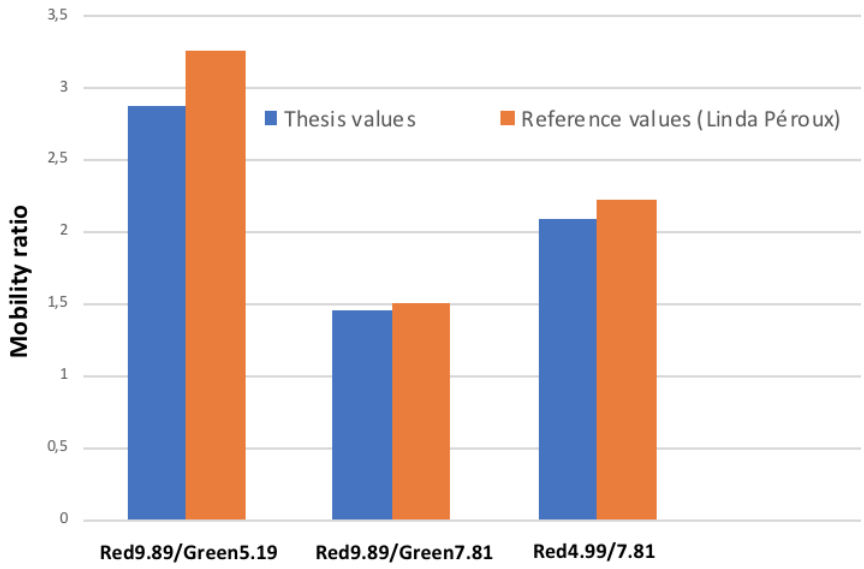

Figure 3.6: Showing the comparison between different measurements of the mobility ratio. Orange color represents reference values (from Linda Péroux) and blue color represents mobility ratio values obtained for this thesis.

3.3 Discussion

For the discussion, a summary of the mobility ratios that were obtained for the different Polystyrene particles are concluded in table 3.5 below.

Table 3.5: Summary of the mobility ratios for the Polystyrene particles that were obtained from the experiments.

Particle type	Buffer	Mobility ratio
9.89μm/7.81μm	MQ	1.45
9.89μm/7.81μm	20% Iodixanol	1.51
4.99μm/7.81μm	MQ	2.09
4.99μm/7.81μm	20% Iodixanol	2.08
9.89μm/5.19μm	MQ	2.87
9.89μm/5.19μm	20% Iodixanol	3.18

From the particle separation there could not be seen a big difference between MQ water and 20% Iodixanol for the run with the red 4.99μm/green 7.81μm. This suggest that the MQ water and 20% Iodixanol seems to have a similar impact on the particles.

A difference was seen for the red 9.89μm and green 5.19μm Polystyrene particles and for the 9.89μm/green 7.81μm Polystyrene particles , where the mobility ratio was higher using 20% Iodixanol rather than MQ water. This indicates that a better separation can be achieved using a solution of 20% Iodixanol. It also indicates that they may have different material properties despite the fact that they share the same composition.

Moreover, it could be seen that there was a little difference if taking the average mobility ratio (average of all data points) compared the analysis based on the quadratic fit (average of the maximum data points). How ever, the same conclusions as above applies for both analysis methods.

Due to the very low concentration used (0.0025% w/v) it was challenging to identify the streamlines properly when doing the MATLAB analysis. Though, it would not be good to increase the concentration too much since this leads to hydrodynamic interactions between the particles because they would be more close to each other. Also, a too high concentration appears to obstruct particle separation. A concentration of 0.001% is found to be a good reference for the Polystyrene particles (Péroux, 2022). New for this thesis work is that the Polystyrene particles are tested in 20% Iodixanol. Since this buffer media has a higher density, there was some problem with clogging in the pipes, and the time for the system to tune in was occasionally long. Beside the need for a more efficient cleaning of the set-up and of the pipes, it was not more difficult to use 20% Iodixanol as a buffer medium compared to MQ-water.

Regarding the fiber in the chip, it seems like the impact of it is was low. If comparing the run with the fiber (red 9.89μm green 7.81μm) with Linda's run for the exact same particles the results are approximately the same. This indicates that result should be reliable even with the fiber in the outlet fork. Otherwise, the results from this thesis and Linda's results agree. There is a small variation in the mobility ratio, mainly the mobility ratio for the red 9.89μm particles and green 5.19μm particles, which can be explained by the way of analysing, concentration of particles and other flow control settings.

4 Separation of cell lines

The main goals of this chapter is to measure the mobility ratio of different of cell lines with respect to different fluorescent Polystyrene particles, to assess their mobility in different buffers. In this thesis experiments are done with DU-145, MCF-7 and Jurkat cell lines. The DU-145 and MCF-7 cell lines are cultivated from the beginning of the thesis and prepared for experiments by hand in cell laboratory.

The Jurkat cell line is obtained from the company AcouSort which has cultivated and prepared the cell line for experiment.

4.1 Cancer and cell lines

Cancer is a common disease and is treated successfully today in many cases. The reason for this is many years of research and gained knowledge about cell metabolism and clinical chemistry. Additional to treatment with chemotherapy and radiation, there are new treatments under development, e.g. CAR T-cells. Treatment with engineered CAR T-cells is when blood is drawn from a patient to isolate the T-cells. In the laboratory, the T-cells are modified with receptors that later is expressed on the surface (engineered chimeric antigen receptor) of the T-cell. This CAR T-cell can then recognize the cancer cells better, and destroy them. They are then grown to large numbers and re-infused into the patient. This technique has been used successfully for treatment of blood cancers like leukemia, lymphomas and multiple myeloma (Institute, 2022).

Cancer occurs when cells starts mutate and to grow and divide in an uncontrollable and in an abnormal manner. Due to the rapid proliferation, the cancer cells has a high requirement of energy and nutrients. The formed cancer cells can in turn form tumors which can be spread to other parts of the body. The process of which tumor cells are spread is called metastasis. As a rule, treatment in a metastatic state is usually less successful and is more of a life-extending treatment. The most common type of cancer in men is prostate cancer. For women, breast cancer is the most common cancer disease (National Cancer Institute: Surveillance and Program, 2019).

In this thesis DU-145, MCF-7 and Jurkat cell lines will be examined. DU-145 cell line is a prostate cancer cell line and MCF-7 cell line is a breast cancer cell line. The DU-145 and MCF-7 cell lines both grow adherent and is $\approx$ 20-25μm in size. A microscopic view of these cell lines can be seen in figure 4.1

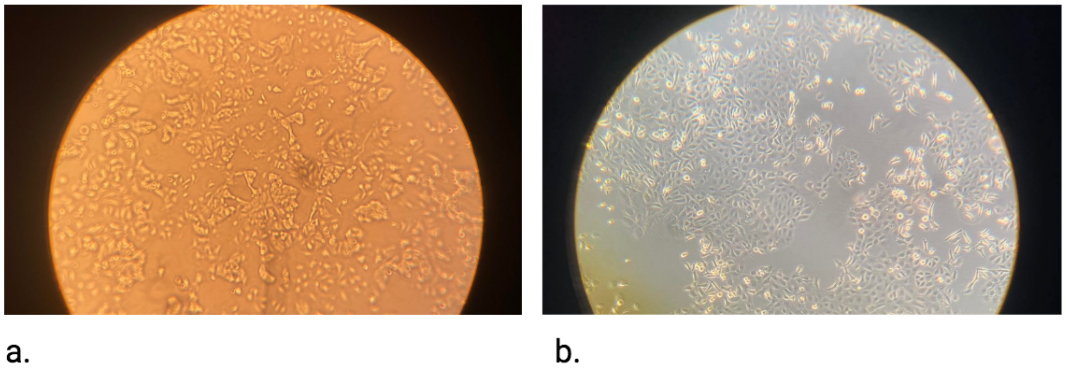

Figure 4.1: a. Showing the MCF-7 cell line in microscopic view b. And the DU-145 cell line. Both of them have adherent growth properties.

The Jurkat cell line is obtained from AcouSort AB and is cultured and prepared by the company. It is an immortalized T-lymphocyte cell line and used in research to gain knowledge about T-cell signaling and cancer. It is a human cell line and has a size of $\approx$ 10-16μm, and was first derived from boy with T-cell leukemia (Yang et al., 2019).

4.2 Cell culture and handeling

The DU-145 and MCF-7 cell lines are cultivated in cell laboratory under standard cell culturing. The cells are constantly suspended in cell culture media, which provides the cells with nutrients and a suitable environment for survival and growth. The cell culture media is changed regularly to create the best conditions for the cells, and consists of nutrients customized for the specific cell type, antibiotics and anti-fungi treatment. Since cells grow fast in good conditions, a splitting process is needed once a week in order to be in control over the number of cells.

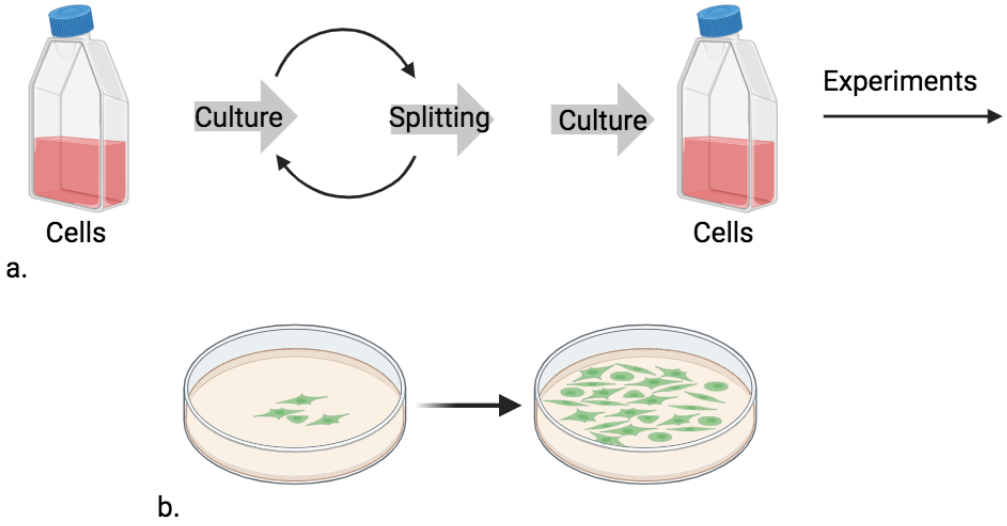

Figure 4.2: a. Rough illustration over the cell culturing process. The process switches between only changing the cell medium and cell splitting. After splitting, incubation in culture medium is needed in order to grow the cells to a reasonable amount before experiment b. Illustration of an desirable growth after the splitting of cells. The growth in the illustration is adherent.

When performing cell splitting, the cell medium is firstly removed by a pipette. Then, there is a cleaning step to remove leftovers of the cell growth medium before trypsin is added. Since the grow properties of the DU-145 cells is adherent, the proteolytic enzyme Trypsin is needed in order to deattach them from the flask and enable splitting of the cells. To neutralize the Trypsin, growth medium is added. The cells are then splitted in order to have a moderate control over the growth and incubated with new cell medium.

When preparing for experiments, the cells are stained in order to be visible in the camera. The goal is to see the cells clearly when illuminated with fluorescent light. For this, Calcein AM is used. Cells are incubated with 7μl Calcein AM for approximately 30 minutes. The unbound Calcein AM is washed away, and the colored cells are suspended in buffer, showing a green color when illuminated with the fluorescent light.

4.3 Method

The set-up used is explained in chapter 1.3, and the flow control settings are kept constant as described in table 4.1.

Table 4.1: Parameters that are used during the experiments with the different cell lines.

Parameter	Value
r_{in}	0.8
r_{out}	0.2
Flow Rate [μl/min]	50
Camera Exposure Time [s]	1-4
Temperature [C°]	25-30

The exact cell concentration was not checked as it varies a bit from batch to batch due to biological reasons. However, an estimate is that approximately 1-2 million cells are harvested from a petri dish. Then some minor losses will occur in the washing and staining procedures before the experiments depending on the operator.

After staining of the cells, the stained cells are diluted with 1 mL chosen buffer and 10μl Polystyrene particles of chosen size are added. This gives approximately 1-2 million cells per mL. The sample is then mixed gentle to be sure that the cells and particles are evenly distributed through the sample tube before running the experiment.

During the experiments the frequency in the main channel is held at approximately 2 MHz (1.996) and in the prefocusing channel 5 MHz (4.89). The amplitude is held constant to 2.5 V in the prefocusing channel whilst the amplitude is switched in the main channel through out the experiment. Which amplitudes that are used for a specific trial is specified with the particular experiment.

Three images were taken for each voltage at the outlet and three images at 0V both at the inlet and outlet to make sure nothing changed during the run. The figures were then measured according to chapter 2.3.1, and further analysed in MATLAB in order to achieve the mobility ratio.

The flow rate used with cells is very low (50 μl/min). Due to the low flow rate, the pressure driven system could be unstable at the beginning. This could occur especially when using Iodixanol as buffer. This problem is somehow overcome by increasing the flow rate to 200 μl/min a few seconds and then decrease it to 50 μl/min again.

4.4 Results and discussion

Below the results for the tests with the different cell lines are presented and discussed.

4.4.1 DU-145 cell line

The mobility ratio of the DU-145 cells with respect to two different Polystyrene particles: red 9.89μm and red 7.81μm is assessed in three different buffers: 0, 10 and 20% Iodixanol. The camera exposure time is held at 1 second.

4.4.1.1 Separation with DU145 and 9.89μm Polystyrene particles

The Polystryene particles used in this experiment are red 9.89μm particles. For the PBS buffer the voltage in the main channel is swept between 0 and 5.5V, for the buffer with 10% Iodixanol it is swept between 0 and 10.5V and for the buffer with 20% Iodixanol it is swept between 0 and 14V.

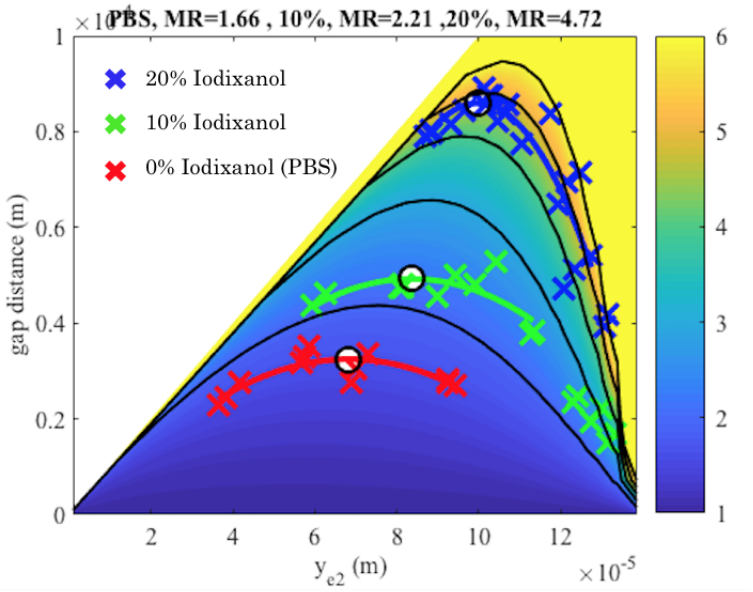

Figure 4.3: Showing the separation curve with a comparison between the three different buffers used: 0, 10 and 20% Iodixanol. The highest gap distance and hence highest mobility ratio is given when using a buffer with 20% Iodixanol. The black circle in respective fitted curve represents the maximum gap distance value.

From the separation curve plot the mobility ratios for each of the buffers were estimated, see below in table 4.2.

Table 4.2: Showing the mobility ratios for three different buffers with DU145 cell and red 9.89μm Polystyrene particles (9.89μm/DU-145). The maximum and minimum mobilities can be seen as the band gap in which the mobility ratio differs in.

% Iodixanol	Mobility ratio	Max Mobility ratio	Min Mobility ratio
0	1.66	1.77	1.54
10	2.21	2.69	2.12
20	4.72	6.07	3.49

To see if there is any difference in the result when using filtering for the analysis in MATLAB, a further comparison was done for the test with 10% Iodixanol: with and without filtering. The filtering is based on least mean squares algorithm. This gave a better view of the cell/particle streams and hence provided better conditions for an accurate measurement. A picture from the channel without filtering is shown in figure 4.4, and the intensity profile without filtering is shown in figure 4.5 and with filtering

in figure 4.6. A view of the cells and particles using filtering is shown in figure 4.7 and 4.8.

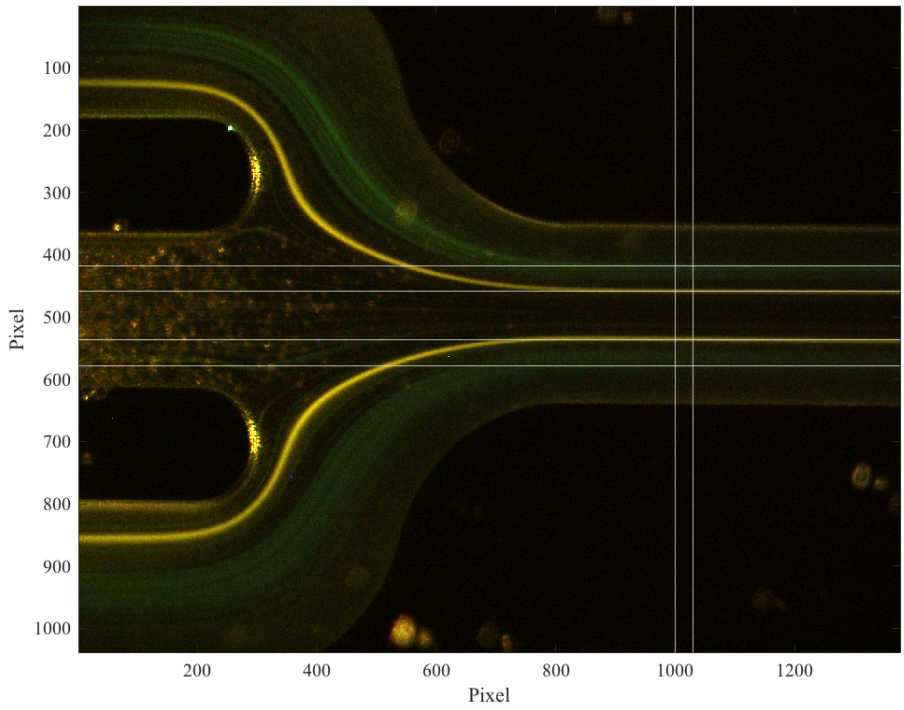

Figure 4.4: Showing the outlet fork at 5V for Calcein AM green stained DU-145 cells and the red 9.89μm Polystyrene particles before filtering. The flow rate used is 50μml/min and rin=0.8 and rout=0.2. The white lines represents the $y_{e1,2}$ positions for the particles/cells. The points where the white lines meet represents the pixel values used for calculating the mobility ratio. The intensity profile without filtering is shown below in 4.5 and with filtering in 4.6.

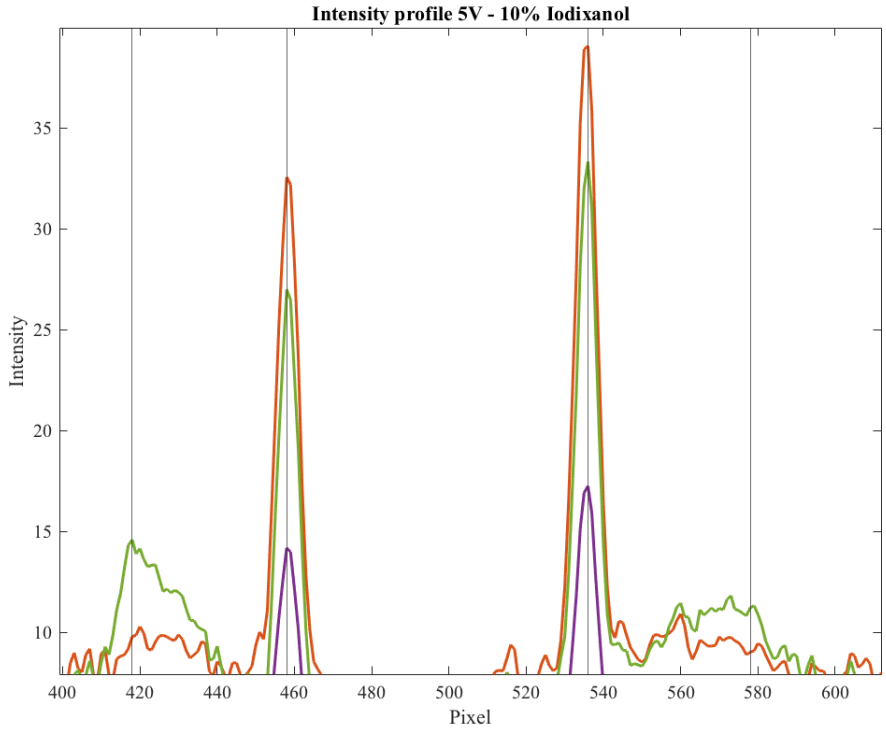

Figure 4.5: Showing the intensity (fluorescent) profile at 5V for the outlet fork using 10% Iodixanol without filtering. The red peaks represents the 9.89μm red particles and the green peaks represents the DU145 cells. The purple curve represents the average.

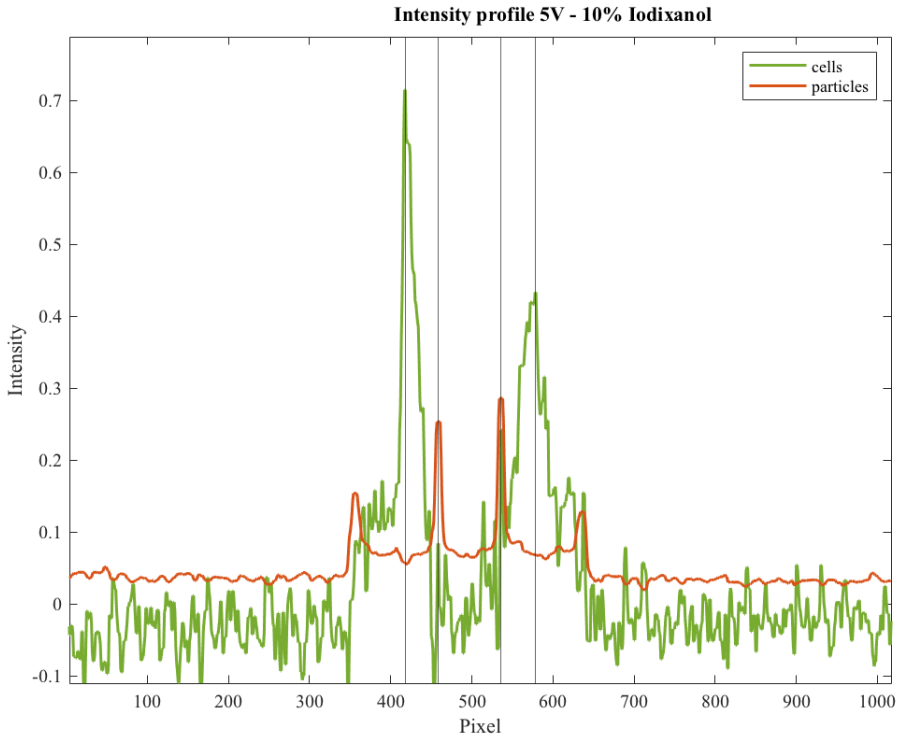

Figure 4.6: Showing the intensity (fluorescent) profile at 5V for the outlet fork using 10% Iodixanol using filtering. The red peaks represents the 9.89μm red particles and the green peaks represents the DU145 cells.

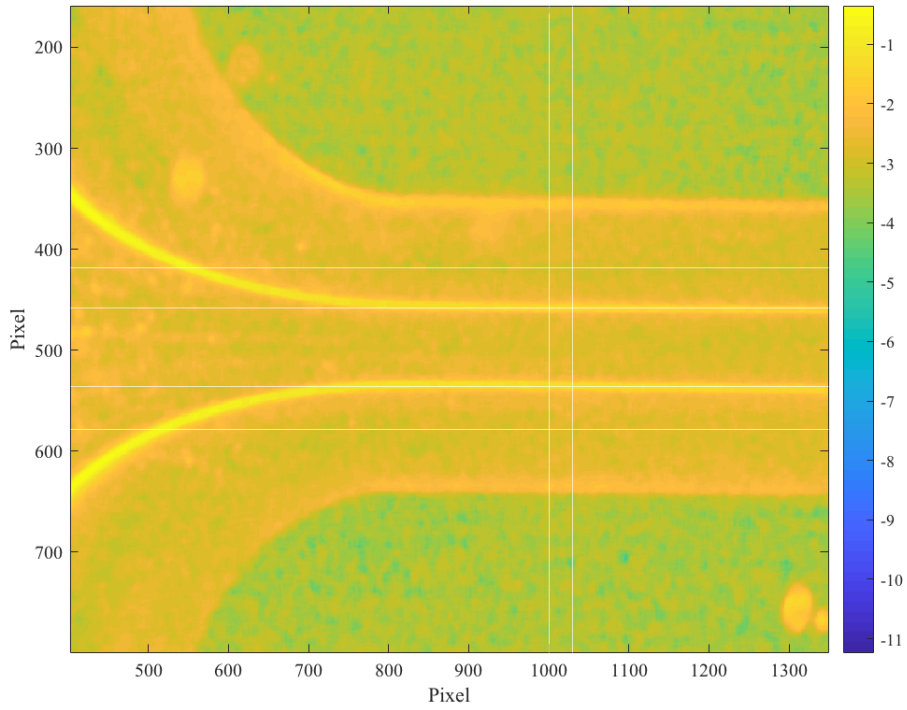

Figure 4.7: Showing the outlet fork at 5V using 10% Iodixanol. The two particle streams representing the 9.89μm Polystyrene particles can be seen clearly using filtering. The flow rate used is 50μml/min and rin=0.8 and rout=0.2.

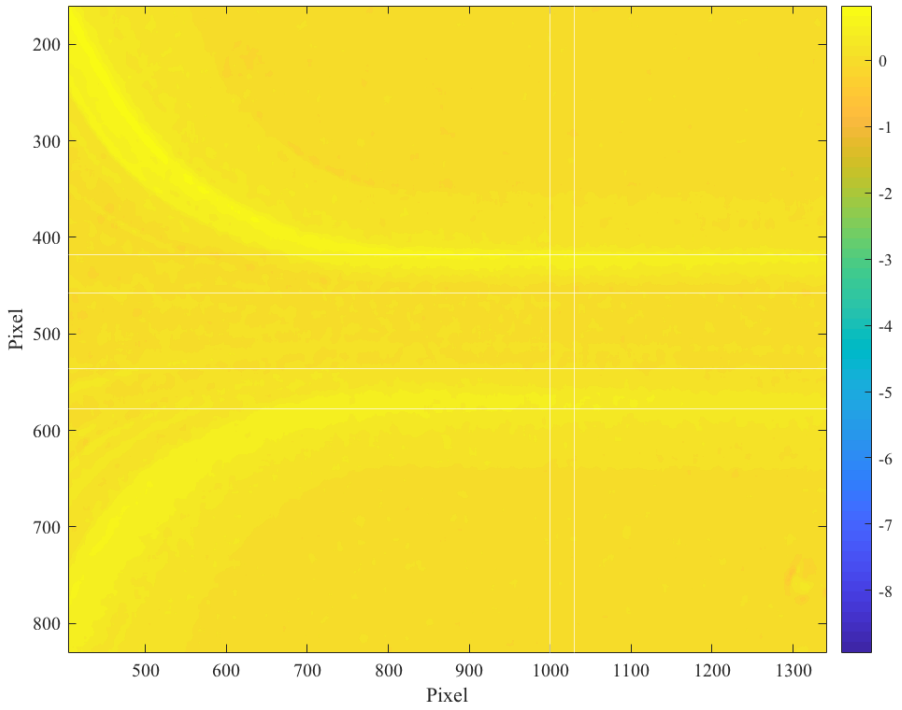

Figure 4.8: Showing the outlet fork at 5V using 10% Iodixanol. The two cell streams representing the DU145 cells can be seen more clearly. As cells behave differently than particles, they are seen to be more spread. The flow rate used is 50μml/min and rin=0.8 and rout=0.2.

After analysing the figures of the DU-145 cells with the red 9.89μm Polystyrene particles in 10% Iodixanol with the new method using filtering, a comparison is done with the analysis method not using filtering. The result is present below in figure 4.9, table 4.3 and table 4.4.

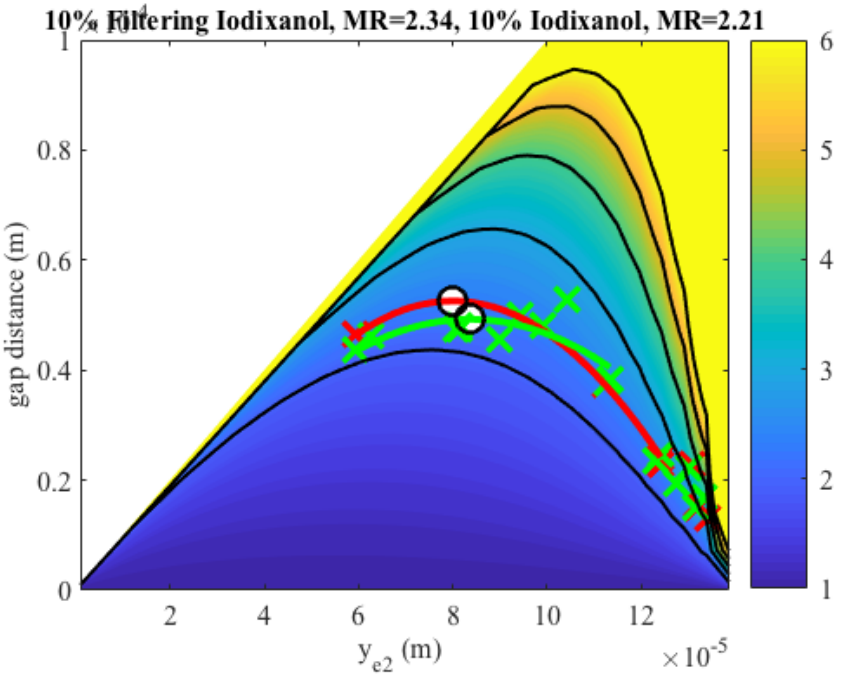

Figure 4.9: Showing the two different separation curve for DU-145 cells and red 9.89μm Polystyrene particles in 10% Iodixanol. The red curve represents the analysis with filtering and the green curve represents the analysis without filtering. For the analysis with filtering less data points are used in the plot.

Table 4.3: Stating the mobility ratios for DU-145 cells and red 9.89μm Polystyrene particles (9.89μm/DU-145) in 10% Iodixanol using analysis *with* filtering.

% Iodixanol	Mobility ratio	Max Mobility ratio	Min Mobility ratio
10	2.34	2.49	2.27

Table 4.4: Stating the mobility ratios for DU-145 cells and red 9.89μm Polystyrene particles (9.89μm/DU-145) in 10% Iodixanol using analysis *without* filtering.

% Iodixanol	Mobility ratio	Max Mobility ratio	Min Mobility ratio
10	2.21	2.69	2.12

4.4.1.2 Separation with DU145 and 7.81μm Polystyrene particles

The mobility ratio between the red 7.81μm Polystyrene particles and the DU-145 cells is assessed in two different buffers: PBS and 10% Iodixanol. For the PBS, the voltage in the main channel is swept between 9 and 14V in steps of 0.5-1V and for the 10% Iodixanol it was swept between 4 and 9V in steps of 0.5-1V. In this run, there was a fiber located at the outlet fork, see figures in Appendix C

Below in figure 4.10 the separation curve is shown and in table 4.5 the mobility ratios for respective run are presented.

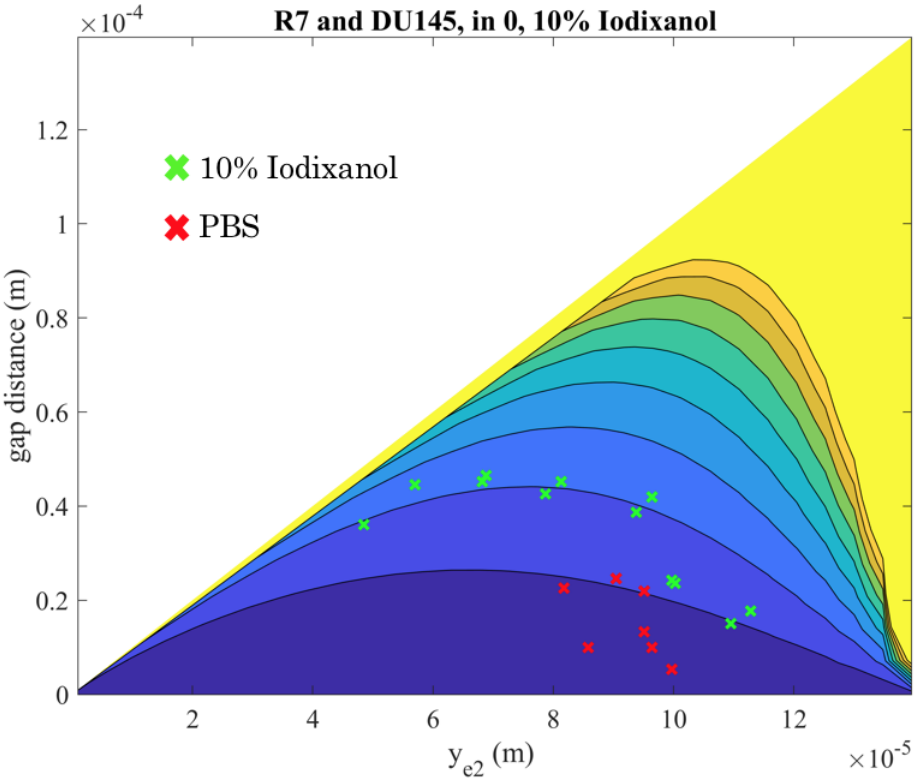

Figure 4.10: Showing the separation curve for the DU145 cells and the red 7.81μm Polystyrene particles in two different buffers: PBS and 10% Iodixanol. This separation curve is *not* plotted due to quadratic fit. Hence, an average of all the data points are used.

Table 4.5: Stating the mobility ratios obtained for the DU145 cells and the red 7.81μm Polystyrene particles in PBS and 10% Iodixanol (7.81μm/DU-145).

% Iodixanol	Mobility ratio
0	1.56
10	2.14

4.4.1.3 Discussion

For the separation between the DU-145 cells and the 9.89μm Polystyrene particles it is shown that the use of a buffer with 20% Iodixanol increases the mobility ratio. The lowest mobility ratio was seen using PBS as a buffer. What can be concluded from this is that as the percentage level of Iodixanol increases from 0 to 20%, the mobility ratio increases, giving a better separation.

The separation between the DU-145 cells and the red 7.81μm Polystyrene particles was tested in two different buffers: PBS and 10% Iodixanol. It was shown that the separation efficiency was better when using 10% Iodixanol rather than using PBS. However, there was a fiber located at the outlet fork which could potentially have

affected the result. Further, there was also clogging of cells which can be seen in in the figures shown in Appendix C. This could to some extent be solved by rinsing with FACS rinse and FACS clean.

It can also be concluded that the separation is slightly better using the red 9.89μm Polystyrene particles with the DU-145 cells rather than the 7.81μm Polystyrene particles. This conclusion can only be drawn when using PBS or 10% Iodixanol since 20% Iodixanol never was tested for the red 7.81μm Polystyrene particles.

For the analysis of the impact of filtering when analysing the figures, comparison was only done for one buffer: 10% Iodixanol. It showed that the mobility ratio was 2.34 when analysed with filtering and 2.21 analysing without filtering. This could indicate that adding the filtering process to the evaluation could make the measurement and analysis more accurate. However, it also shows that the analysis tool works quite appropriate even though there are few data points used. It would be good to re-do this comparison between more experiments to see if it is a coincidence or if it actually is a more efficient way to analyse the data.

4.4.2 MCF-7 cell line

The mobility ratio of the MCF-7 cells with respect to red 7.79μm Polystyrene particles is assessed in three different buffers, 0, 10 and 20% Iodixanol. Camera exposure time is altered between 3-4 seconds. The frequency in the pre-focusing channel is set to 4.89 MHz with a constant amplitude at 2.5V. The frequency in the main channel is set to 1.996 MHz and the amplitude is altered differently between the different runs.

4.4.2.1 Separation of MCF-7 and 7.79μm Polystyrene particles in PBS

During this run it was hard to see the cells clearly, which made the analysis more difficult. The amplitude in the main channel was swept between 0 and 1V with small steps of 0,1-0,2V.

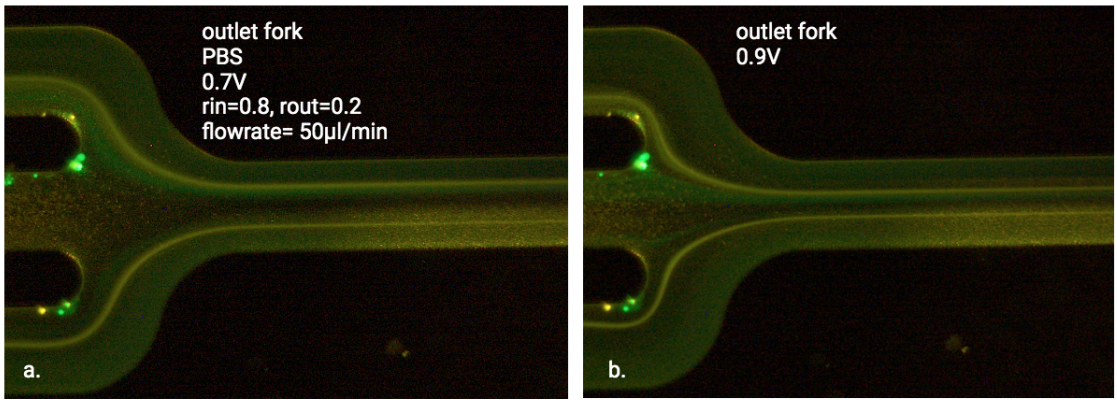

Figure 4.11: a. The outlet fork at 0.7V with red 7.79μm Polystyrene particles and Calcein AM stained cells (green). Cells are seen weakly b. The outlet fork at 0.9V. Cells are entering the center outlet and particles on the side outlet. The Calcein AM green stained MCF-7 are separated from the red 7.79μm Polystyrene particles.

A separation curve for the run was obtained, see figure 4.12 below. A mobility ratio of 1.5 for the 7μm (7.79) Polystyrene particles and MCF-7 cells in PBS was obtained (MCF-7/7.79μm).

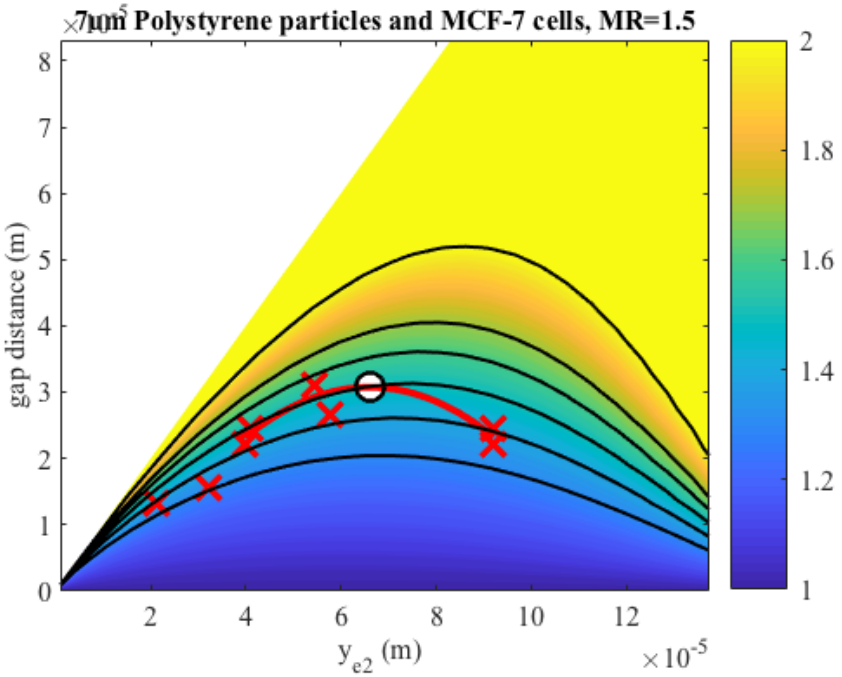

Figure 4.12: Showing the separation curve for the 7μm polystyrene particles and MCF-7 cells, giving a mobility ratio of 1.5.

4.4.2.2 Separation of MCF-7 and 7.79μm Polystyrene particles in 10 and 20% Iodixanol

During the experiment with 10% Iodixanol the cells were difficult to see. The amplitude in the main channel was swept between 0 and 2V. When reaching 1.5-2V, it could be seen clearly that the cells were pushed more and more towards the sides (never to the center) and that the particles are moved to the center, see figure 4.13. The fact that the cells are pushed towards the sides is indicating that they have a negative contrast factor.

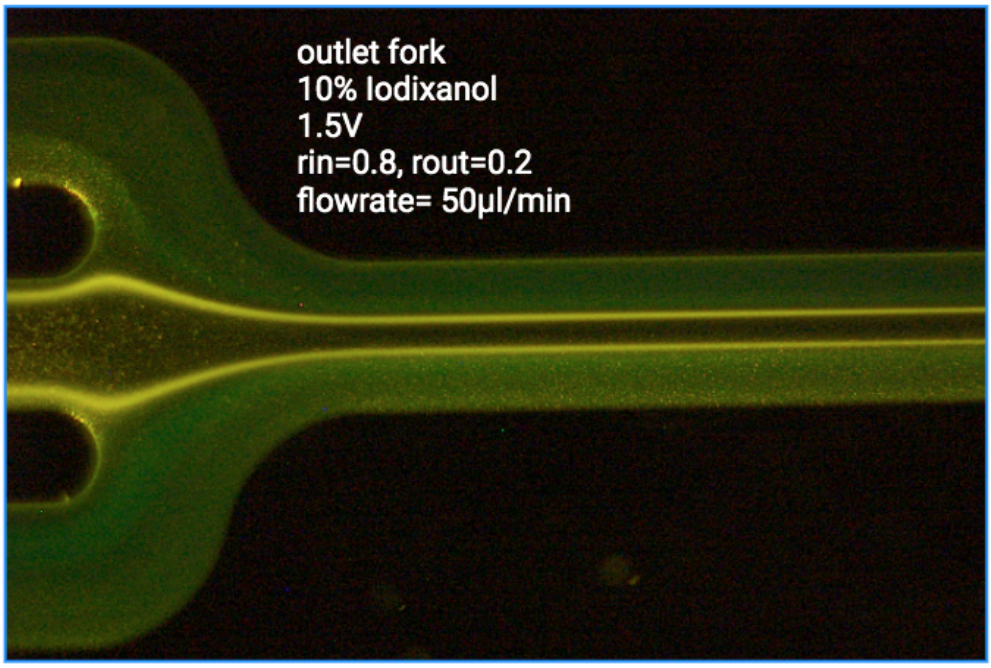

Figure 4.13: Showing the outlet fork at 1.5V for the Calcein AM green stained MCF-7 cells and red 7.79μm Polystyrene particles in a buffer with 10% Iodixanol. Cells are seen poorly (green) and enters through side outlet. Particles (red) enters through center outlet.

For more figures, see Appendix B. In the experiment with 20% Iodixanol the cells were clearly seen. The cells are clearly separated from the particles, and they are pushed to the sides indicating that they have a negative contrast factor, see figure 4.14 below.

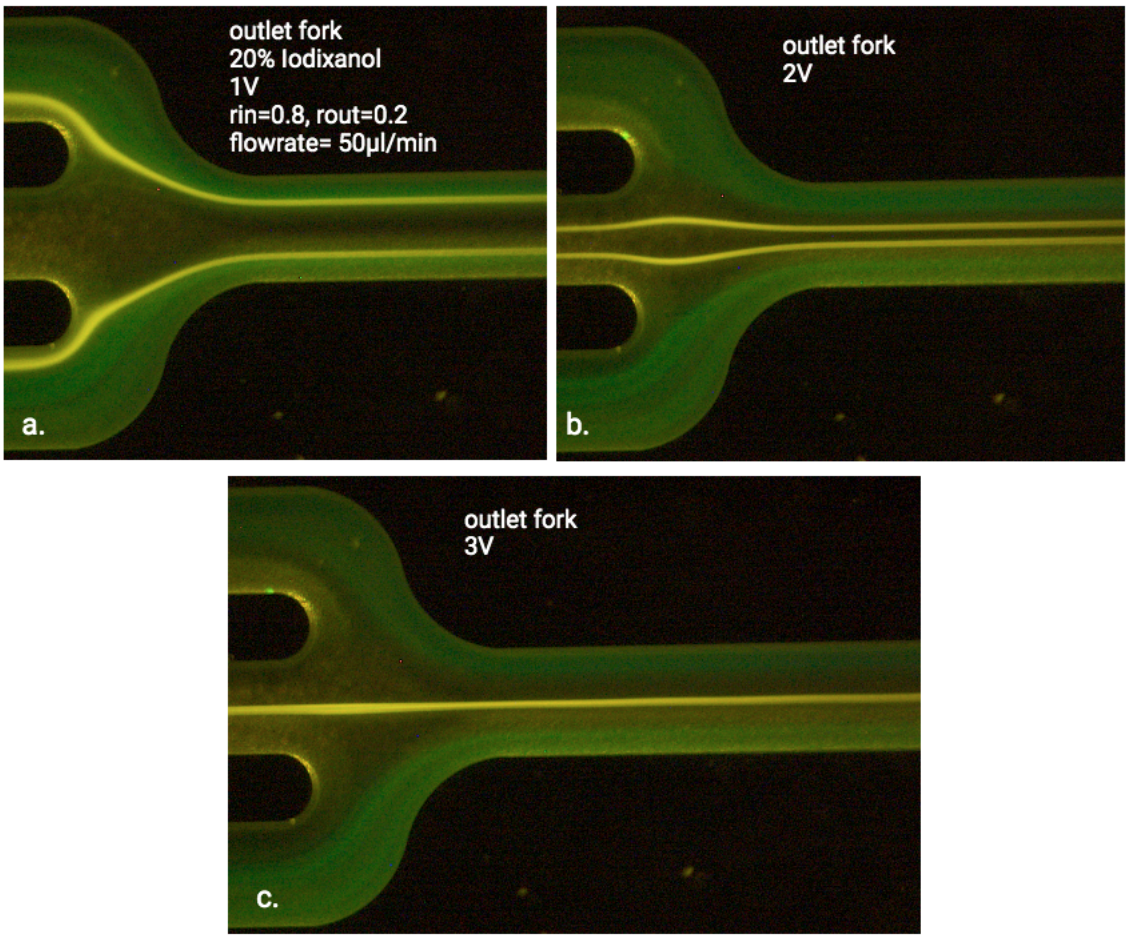

Figure 4.14: a. Showing the outlet fork at 1V b. The outlet fork at 2V, particles moves to the center outlet and cells to side outlet c. The outlet fork at 3V. Cells are pushed to the side, showing that they exert a negative contrast factor.

4.4.2.3 Discussion

The separation between the red 7.79μm Polystyrene particles and the MCF-7 cells were run in three different buffers. The cells were hard to see both in the PBS and the 10% Iodixanol buffer. The reason for the cells to be seen weak during these tests is probably that the amount of cells was a bit low or that the staining concentration should have been a bit higher.

In PBS a mobility ratio of 1.5 (MCF-7/7.79μm) was obtained and for the runs with 10% and 20% Iodixanol it could be seen that the cells exerted a negative contrast factor, pushing the cells to the sides rather into the center. This indicates that the acoustic contrast factor for the cells changes when using a buffer with 10 or 20 % Iodixanol. This enabled a good separation between the 7μm Polystyrene particles and the MCF-7 cells in both these buffers. Due to the switch in contrast factor no analysis was done in MATLAB for the 10 and 20% Iodixanol runs. This is since the analysis method is not developed to take a negative contrast factor into account.

4.4.3 Jurkat cell line

The mobility ratio of the Jurkat cells with respect to red 7.79μm Polystyrene particles is assessed in three different buffers, 0,10 and 20% Iodixanol. The camera exposure time is altered between the different trials to be able to see the cells better, due to the variation of cells in the sample tube. The frequency in the pre-focusing channel is set to 4.89 MHz with a constant amplitude at 2.5V. The frequency in the main channel is set to 1.996 MHz and the amplitude is altered differently between the different runs, see below for a specific run.

4.4.3.1 Separation of Jurkat cells and 7.79μm Polystyrene particles in PBS

For the run with PBS as a buffer the amplitude in the main channel was swept between 0 and 4V with steps of 0.5-1V in the main channel. The camera exposure time was held to three seconds. There was no very clear separation between the cells and particles using PBS as buffer, see figure 4.15 below.

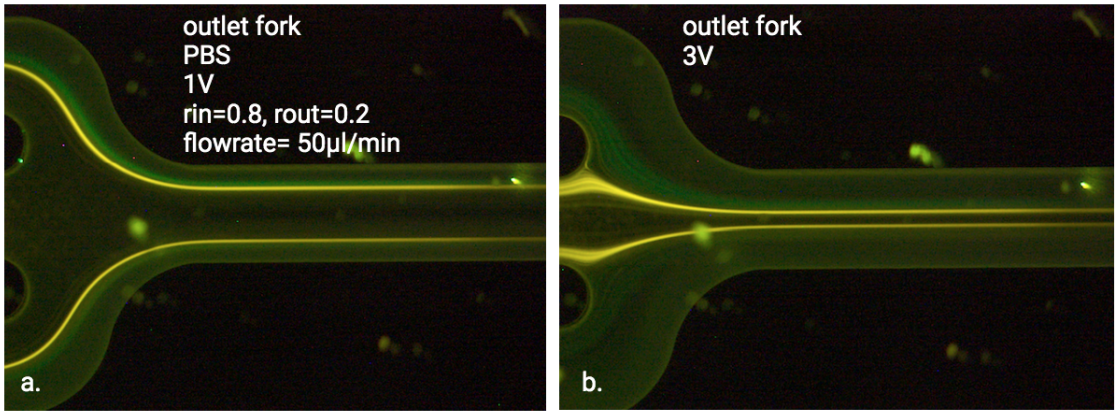

Figure 4.15: a. Showing the outlet fork at 1V for the Calcein AM green stained Jurkat cells and the red 7.79μm Polystyrene particles in PBS b. Outlet fork at 3V, showing that the two streamlines (cells and particles) follows each other rather tightly - no clear separation.

The separation curve obtained is shown in figure 4.16 below. A mobility ratio of 1.57 (7.79μm/Jurkat) was obtained.

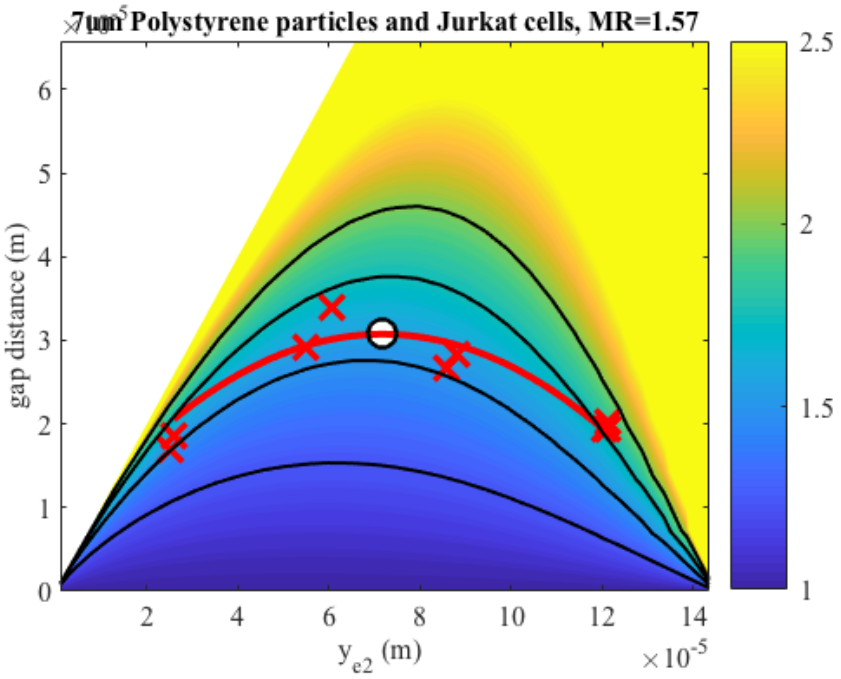

Figure 4.16: Showing the separation curve for the red 7.79μm Polystyrene particles with Jurkat cells in 0% Iodixanol (PBS). The mobility ratio is estimated to 1.57 (7.79μm/Jurkat).

4.4.3.2 Separation of Jurkat cells and 7.79μm Polystyrene particles in 10% Iodixanol

For the run with 10% Iodixanol as buffer, the amplitude in the main channel was swept between 0-4.5V. The camera exposure time was altered between 3-4 s. When reaching 3V in the main channel a clear separation between the particles and cells could be seen, see below in figure 4.17.

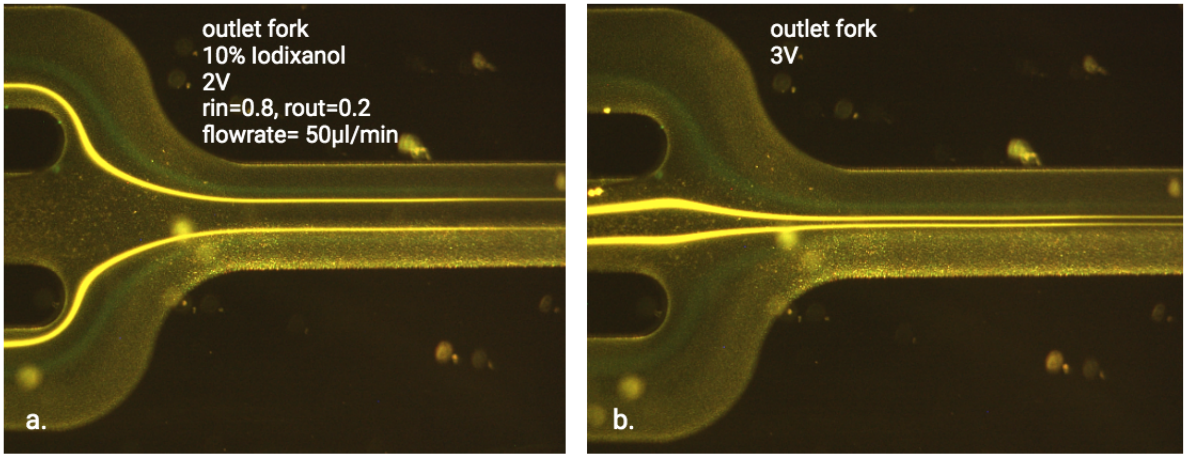

Figure 4.17: a. Showing the outlet fork at 2V for the Calcein AM green stained Jurkat cells and the red 7.79μm Polystyrene particles in 10% Iodixanol b. And the outlet fork at 3V. A clear separation between the cells (green) and particles (red) can be seen.

The separation curve that was obtained is shown below in figure 4.18. A mobility ratio of 2.2 (7.79μm/Jurkat) was obtained.

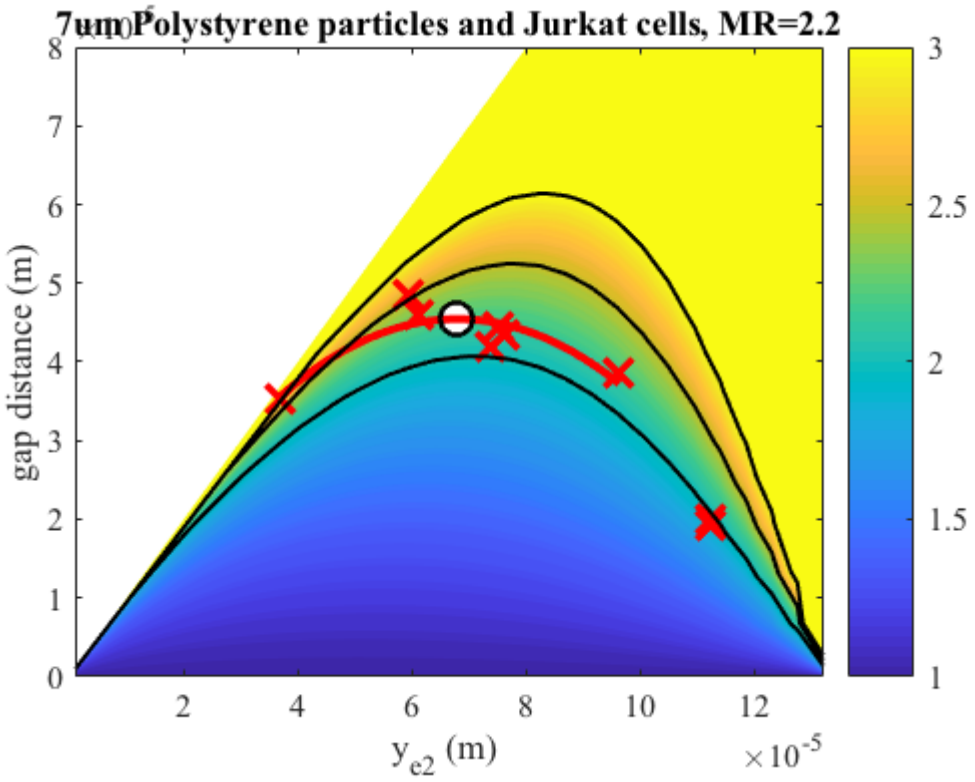

Figure 4.18: Showing the separation curve for the red 7.79μm Polystyrene particles with Jurkat cells in 10% Iodixanol. The mobility ratio is estimated to 2.2 (7.79μm/Jurkat).

4.4.3.3 Separation of Jurkat cells and 7.79μm Polystyrene particles in 20% Iodixanol

For 20% Iodixanol the amplitude in main channel was swept between 0 and 5.5V. When reaching 3-3.5V a clear separation between the 7μm polystyrene particles and Jurkat cells could be seen, see figure 4.19 below. The camera exposure time was altered between 3-4s.

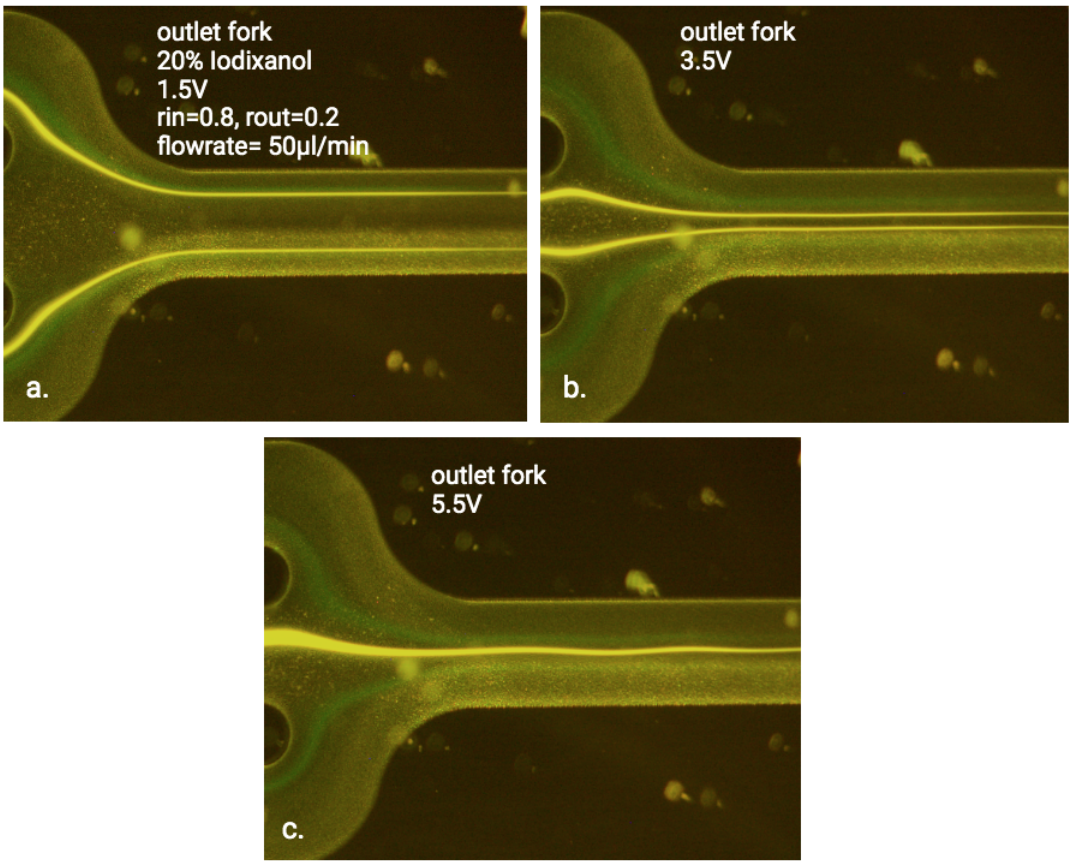

Figure 4.19: a. Showing the outlet fork for the red 7.79μm Polystyrene particles (red) and the Jurkat cells (green) at 1.5V in the main channel with 20% Iodixanol b. The outlet fork at 3.5V, showing a clearly separation between the particles and cells c. The outlet fork at 5.5V, showing a bit instability.

The instability shown in figure 4.19 c. can be explained by that the sample volume was very low at the end of the experiment generating an imbalance in the pressure driven system.

The separation curve obtained for the run can be seen below in figure 4.20. A mobility ratio of 3.05 (7.79μm/Jurkat) was obtained.

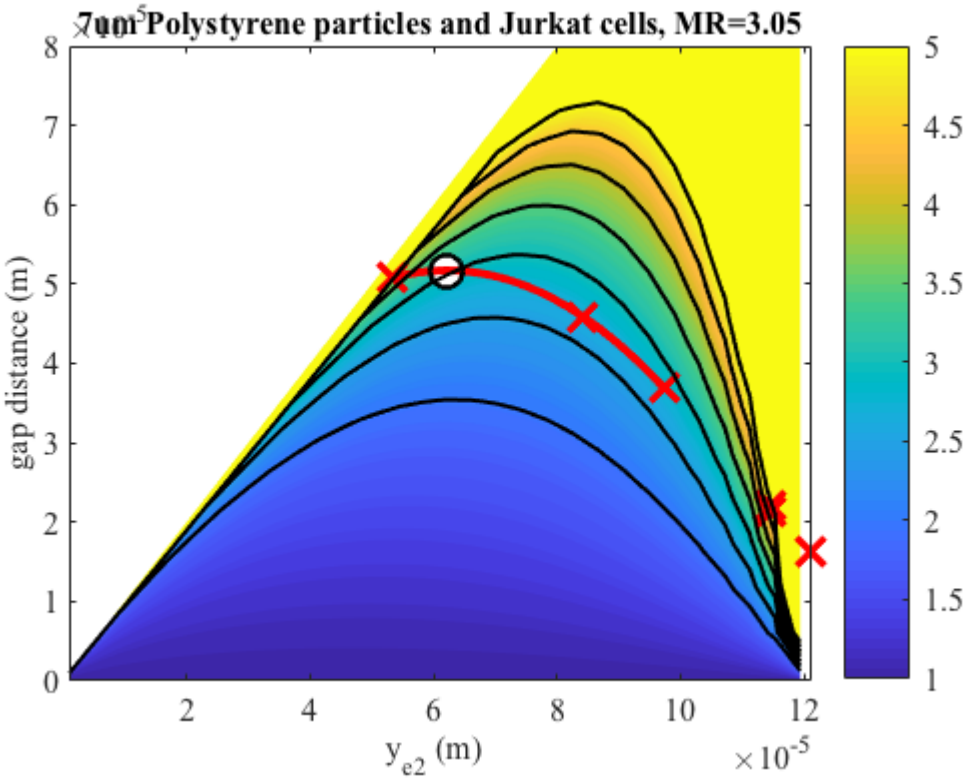

Figure 4.20: Showing the separation curve for the 7μm polystyrene particles with Jurkat cells in 20% Iodixanol. The values of ye2 is plotted as a function of gap distance. The mobility ratio is estimated to 3.05 (7.79μm/Jurkat).

4.4.3.4 Discussion

The highest mobility ratio that was obtained for the red 7.79μm Polystyrene particles with Jurkat cells was 3.05 in a buffer with 20% Iodixanol. The lowest mobility ratio was seen when the sample was in a buffer with 0% Iodixanol (PBS), giving a mobility ratio of 1.57. A higher mobility ratio indicates a better separation, meaning that the separation between the 7.79μm Polystyrene particles and Jurkat cells is more efficient in 20% Iodixanol, and least efficient in PBS.

In both 10% and 20% Iodixanol a clear separation between the cells and particles could be seen.

5 Conclusions and Future Directions

5.1 Overarching conclusions

The foremost goal with this thesis was to measure the mobility ratio between cells and particles within different buffers to assess the separability between different cell-lines. With this came the process of how to cultivate cells and the struggle of getting the set-up to work as long as the cells stayed healthy for experiment. The latter indeed tried the patience, and many times the cells were lost due to problems with the set-up. The change of density between the buffers created problems with the pressure driven system and clogging in the tubing. Also, there was a lot of problem with fiber within the chip which led to the need for the chip to be taken apart and rinsed, which is a time consuming process. Despite this, the outcomes of this thesis considering the thesis goals should be seen as successful.

From the experiments with the Polystyrene particles it can be concluded that the separation between the 4.99μm and 7.81μm particles was equal efficient in MQ water and 20% Iodixanol. Regarding the test with the 9.89μm/5.19μm and 9.89μm/7.81μm Polystyrene particles, the separation was better when using a buffer with 20% Iodixanol. This was also seen in Linda Péroux's work Péroux, 2022, analysing the same Polystyrene particles. This remark suggest that the Polystyrene particles have different material properties, which also is confirmed by (Edthofer et al., 2023). The use of 20% Iodixanol with Polystyrene particles worked fine, though it was found out that it was important to clean the set-up and tubings carefully both before and after experiments to prevent clogging.

The DU-145 cells were tested with two different types of Polystyrene particles: red 9.89μm and red 7.81μm. The best separation were seen when using the DU-145 cells with the 9.89μm Polystyrene particles in PBS and 10% Iodixanol. Regarding the separation with the 9.89μm Polystyrene particles the separation were successful using all of the three buffers: PBS, 10 and 20% Iodixanol. The differences between the separation with 9.89μm and 7.81μm in PBS and 10% Iodixanol are related to the particle properties. The 7.81μm is smaller in size making them travel slower compared to the 9.89μm particles. Regarding the test with the 9.89μm Polystyrene particles in 10% Iodixanol the analysis were done with and without LMS algorithms. There was a small difference in the mobility ratio values, indicating that the filtering possibly contributed to make the measurements more accurate. Also, it could be seen that the estimation of the mobility ratio with only few data point gives a good approximation for the mobility ratio.

General for the trials with MCF-7 cells was that the cells were hard to see. This made the analysis harder but still successful. Three buffers were tested: PBS, 10 and 20% Iodixanol. It was found that the cells changed sign of the contrast factor when used in combination with 10 and 20% Iodixanol. The negative contrast factor of the

cells enabled a good separation between the MCF-7 cells and the 7.79μm Polystyrene particles, where the MCF-7 cells were pushed to the anti nodes entering through the side outlets and the 7.79μm Polystyrene particles through the center outlet.

The best separation between the Jurkat cells and the 7.79μm Polystyrene particles was seen when using a buffer with 20% Iodixanol. Using both 10 and 20% Iodixanol a fully separation from the 7.79μm Polystyrene particles could be seen. This suggest that the separation is good when using a higher density of the buffer since the separation with PBS (0 % Iodixanol) was less efficient.

These results provides information about the different cell lines and how they behave in respect to different types of Polystyrene particles. Since the MCF-7 cells exerts a negative contrast factor in 10% and 20% Iodixanol it should be possible to separate them from the Jurkat and DU-145 cell line. This can be used for further investigations and research within the area since the gained knowledge of their behaviour. Also, a lot of knowledge was gained regarding considering the analysis methods which can contribute to better and more accurate measurements for the mobility ratio, providing a better starting point for the future study of parameters affecting it, such as the buffer media.

5.2 Future aspects

For the future it would be of great importance further analyse the Polystyrene particles and investigate how they differ in material properties. This since they are used a lot in research and are used as a reference when experimenting with cells.

It would also be interesting to see if there is any way to improve the system when e.g operating at low flow rates, such as 50 μl/min as used for the cells. This since it takes some time for the system to tune in which causes unnecessary loss of sample. Due to this, it would also be interesting for the future to experiment with the flow rate when running cells to see if the throughput could possibly be enhanced.

Also it would be interesting to separate different cell lines in respect to each other. Maybe the challenge would be to find a suitable staining method so that both of the cell types can be seen and distinguished.

Bibliography

Edthofer, Alexander, Jakub Novotny, Andreas Lenshof, Thomas Laurell, and Thierry Baasch (2023). "Acoustofluidic Properties of Polystyrene Microparticles". English. In: *Analytical Chemistry*. ISSN: 1520-6882. DOI: 10.1021/acs.analchem.3c01156.

Institute, National Cancer (2022). *CAR T Cells: Engineering Patients' Immune Cells to Treat Their Cancers*.

Jakobsson, Ola, Carl Grenvall, Maria Nordin, Mikael Evander, and Thomas Laurell (2014). "Acoustic actuated fluorescence activated sorting of microparticles". In: *Lab on a Chip* 14.11, pp. 1943–1950.

Laurell, Thomas (2021a). *Acoustophoresis - Migration with sound*. Department of Biomedical Engineering, LTH, Faculty of Engineering.

– (2021b). *Lab exercise instruction – Acoustophoresis*. Thomas Laurell.

Lenshof, Andreas (2008). *Acoustic standing wave manipulation of particles and cells in microfluidic chips*. Andreas Lenshof.

Lenshof, Andreas and Thomas Laurell (2010). "Continuous separation of cells and particles in microfluidic systems". In: *Chemical Society Reviews* 39.3, pp. 1203–1217.

– (2011). "Emerging clinical applications of microchip-based acoustophoresis". In: *JALA: Journal of the Association for Laboratory Automation* 16.6, pp. 443–449.

Li, Peng, Zhangming Mao, Zhangli Peng, Lanlan Zhou, Yuchao Chen, Po-Hsun Huang, Cristina I Truica, Joseph J Drabick, Wafik S El-Deiry, Ming Dao, et al. (2015). "Acoustic separation of circulating tumor cells". In: *Proceedings of the National Academy of Sciences* 112.16, pp. 4970–4975.

Martin, NC, AA Pirie, LV Ford, CL Callaghan, K McTurk, David Lucy, and DG Scrimger (2006). "The use of phosphate buffered saline for the recovery of cells and spermatozoa from swabs." In: *Science & justice: journal of the Forensic Science Society* 46.3, pp. 179–184.

National Cancer Institute: Surveillance, E. and End Results Program (2019). "Cancer stat facts: Common cancer sites". In.

Nilsson, Andreas, Filip Petersson, Henrik Jönsson, and Thomas Laurell (2004). "Acoustic control of suspended particles in micro fluidic chips". In: *Lab on a Chip* 4.2, pp. 131–135.

Péroux, Linda (2022). *Pushing the boundaries of acoustic particle separation: achieving high-throughput, avoiding spillover effects, investigating the effects of the particle concentration, and measuring acoustic properties*. Linda Péroux.

Regmi, Sagar, Chetan Poudel, Rameshwar Adhikari, and Kathy Qian Luo (2022). "Applications of microfluidics and organ-on-a-chip in cancer research". In: *Biosensors* 12.7, p. 459.

Shanko, Eriola-Sophia, Yoeri van de Burgt, Patrick D Anderson, and Jaap MJ den Toonder (2019). "Microfluidic magnetic mixing at low reynolds numbers and in stagnant fluids". In: *Micromachines* 10.11, p. 731.

Song, Peiyi, Rui Hu, Danny Jian Hang Tng, and Ken-Tye Yong (2014). "Moving towards individualized medicine with microfluidics technology". In: *Rsc Advances* 4.22, pp. 11499–11511.

Undvall, Eva, Fabio Garofalo, Giuseppe Procopio, Wei Qiu, Andreas Lenshof, Thomas Laurell, and Thierry Baasch (2022). "Inertia-Induced Breakdown of Acoustic Sorting Efficiency at High Flow Rates". In: *Physical Review Applied* 17.3, p. 034014.

Urbansky, Anke (2019). "Acoustofluidic preparation of whole blood components". In.

Urbansky, Anke, Franziska Olm, Stefan Scheding, Thomas Laurell, and Andreas Lenshof (2019). "Label-free separation of leukocyte subpopulations using high throughput multiplex acoustophoresis". In: *Lab on a Chip* 19.8, pp. 1406–1416.

Yang, Tianhang, Ji Peng, Zhiquan Shu, Praveen K Sekar, Songjing Li, and Dayong Gao (2019). "Determination of the membrane transport properties of Jurkat cells with a microfluidic device". In: *Micromachines* 10.12, p. 832.

Appendix A

Figures Jurkat cells

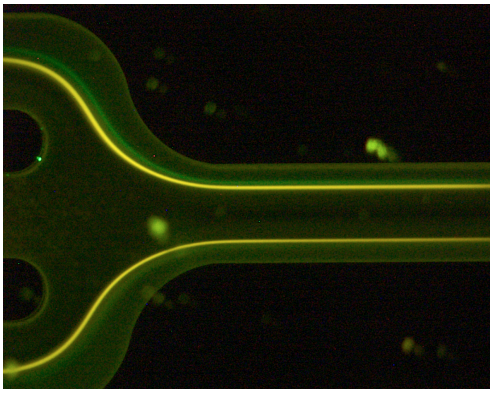

(a) Outlet fork at 1V

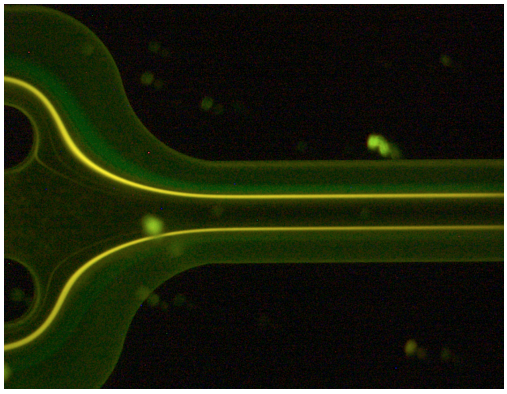

(b) Outlet fork at 1.5V

Figure A.1: Showing the Jurkat cells with the red 7.79μm Polystyrene particles in 0% Iodixanol (PBS). rin=0.8, rout=0.2 and flow rate 50μl/min.

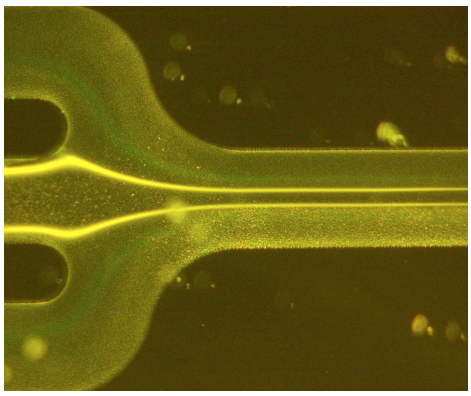

(a) Outlet fork at 2.5V

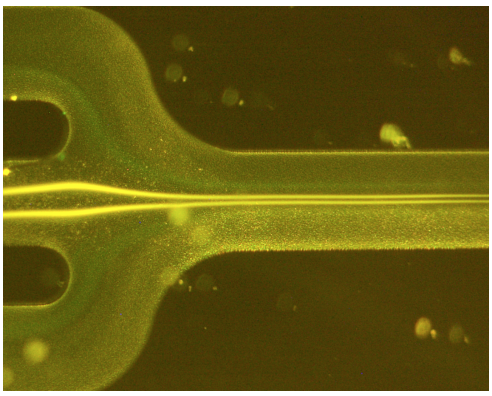

(b) Outlet fork at 3V

Figure A.2: Showing the Jurkat cells with the red 7.79μm Polystyrene particles in 10% Iodixanol. rin=0.8, rout=0.2 and flow rate 50μl/min.

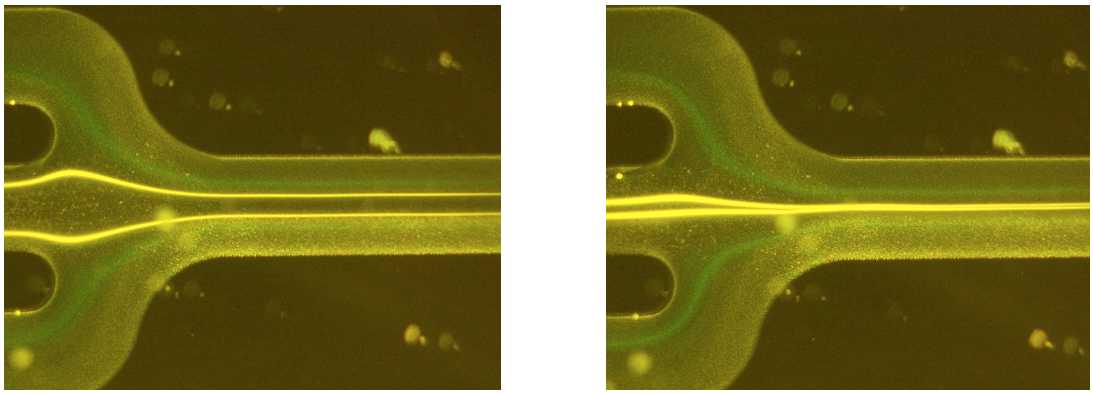

(a) Outlet fork at 3V

(b) Outlet fork at 4.5V

Figure A.3: Showing the Jurkat cells with the red 7.79μm Polystyrene particles in 20% Iodixanol. rin=0.8, rout=0.2 and flow rate 50μl/min.

Appendix B

Figures MCF-7 cells

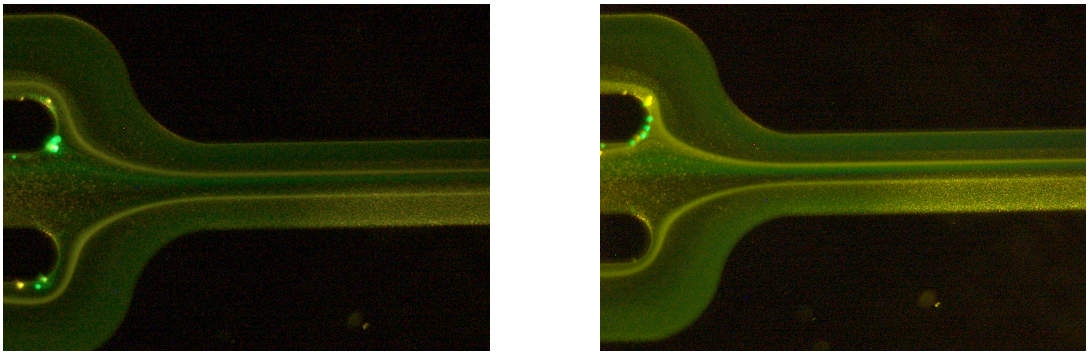

(a) Outlet fork at 0.9V **(b)** Outlet fork at 1V

Figure B.1: Showing the MCF-7 cells with the red 7.79μm Polystyrene particles in 0% Iodixanol (PBS). rin=0.8, rout=0.2 and flow rate 50μl/min.

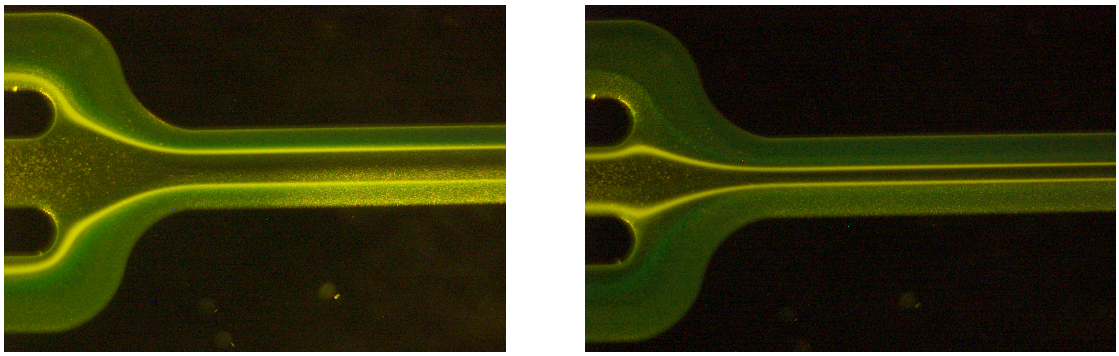

(a) Outlet fork at 1V **(b)** Outlet fork at 1.5V

Figure B.2: Showing the MCF-7 cells with the red 7.79μm Polystyrene particles in 10% Iodixanol. rin=0.8, rout=0.2 and flow rate 50μl/min.

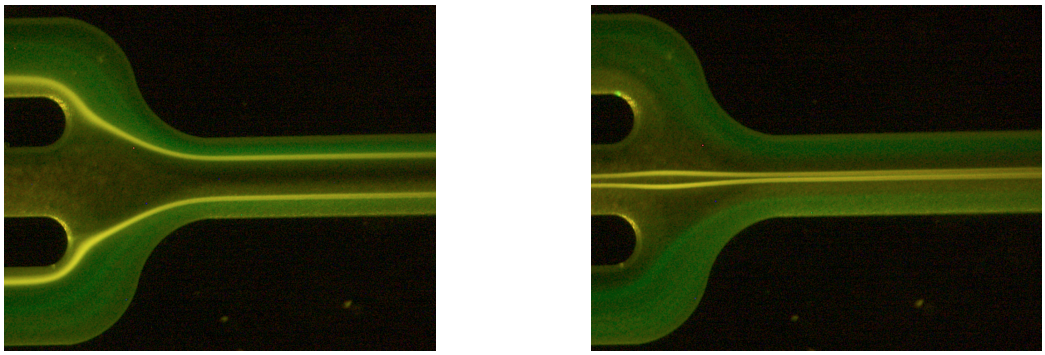

(a) Outlet fork at 1V

(b) Outlet fork at 2.5V

Figure B.3: Showing the MCF-7 cells with the red 7.79μm Polystyrene particles in 20% Iodixanol. rin=0.8, rout=0.2 and flow rate 50μl/min.

Appendix C

Figures DU-145 cells

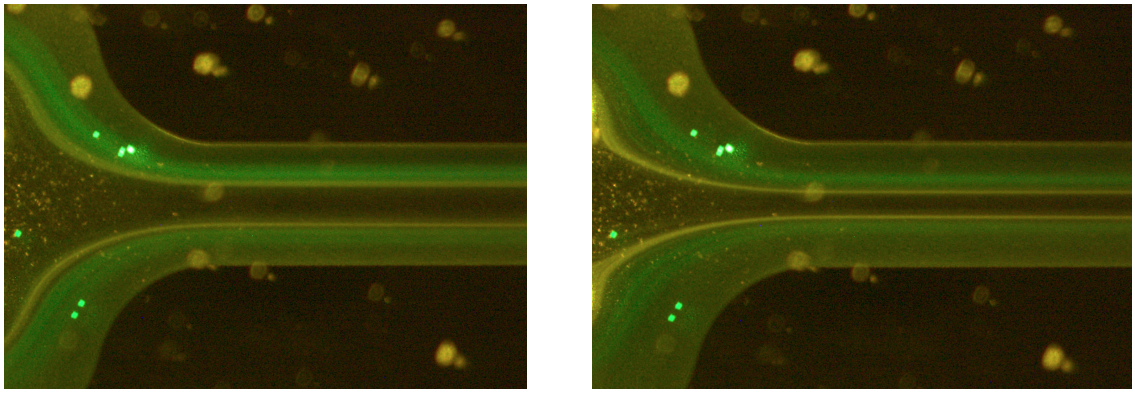

(a) Outlet fork at 3V **(b)** Outlet fork at 3.5V

Figure C.1: Showing the DU-145 cells with the red 9.89μm Polystyrene particles in 0% Iodixanol (PBS). rin=0.8, rout=0.2 and flow rate 50μl/min.

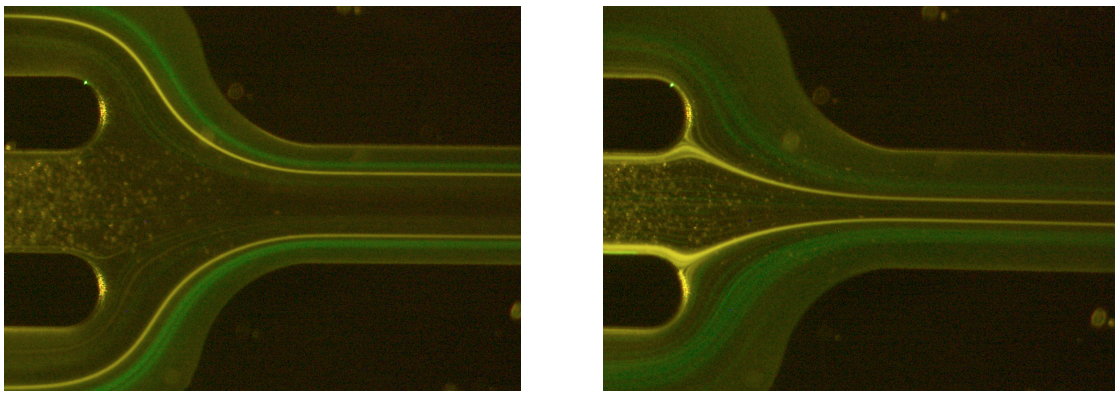

(a) Outlet fork at 3V **(b)** Outlet fork at 6V

Figure C.2: Showing the DU-145 cells with the red 9.89μm Polystyrene particles in 10% Iodixanol. rin=0.8, rout=0.2 and flow rate 50μl/min.

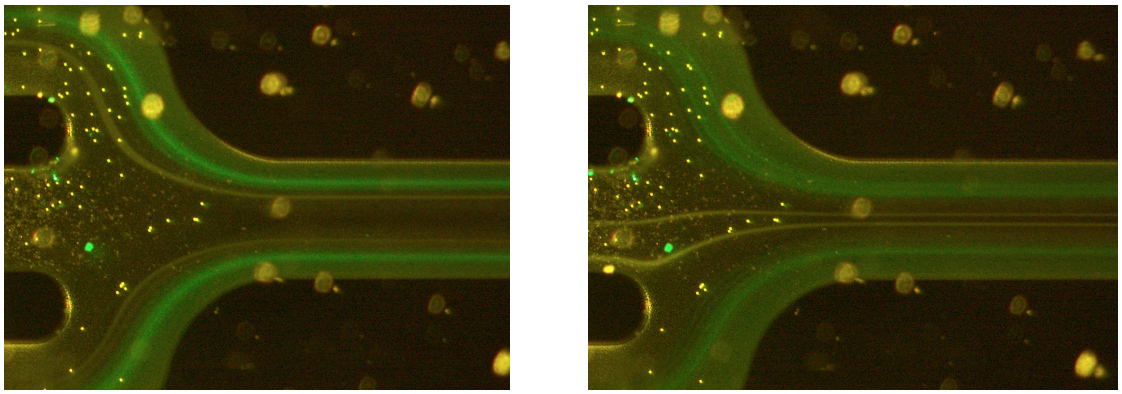

(a) Outlet fork at 4V **(b)** Outlet fork at 6V

Figure C.3: Showing the DU-145 cells with the red 9.89μm Polystyrene particles in 20% Iodixanol. rin=0.8, rout=0.2 and flow rate 50μl/min.

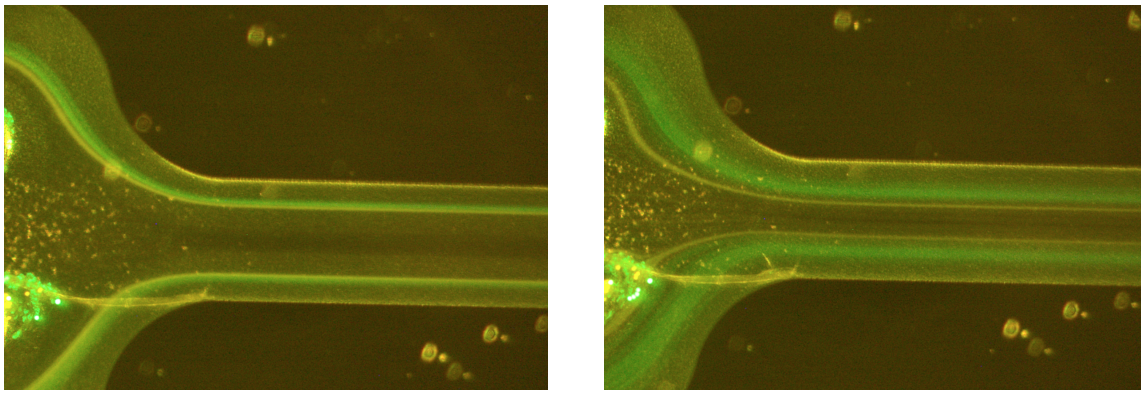

(a) Outlet fork at 3V. Fiber in the outlet. **(b)** Outlet fork at 6V. Fiber in the outlet.

Figure C.4: Showing the DU-145 cells with the red 7.81μm Polystyrene particles in 10% Iodixanol. rin=0.8, rout=0.2 and flow rate 50μl/min.